STUDIES DIRECTED TOWARDS THE PULSING OF THE BEAM OF THE EDINBURGH UNIVERSITY HIGH VOLTAGE PARTICLE ACCELERATOR

Thesis

Submitted by

DAN MAYDAN, Engineer, B.Sc., M.Sc.

for the degree of

DOCTOR OF PHILOSOPHY

University of Edinburgh,
February, 1965.

C O N T E N T S

C O N T E N T S (Contd.)

---

1. INTRODUCTION

1.1. The Aim of the Research

1.1.1. The time-of-flight technique

The study of the neutrons emitted from nuclear reactions may be carried out by a time-of-flight technique. The determination of a particle energy by this method requires the determination of a zero time related to the time at which the particle begins on its flight path. Time interval is measured between the zero time and the instant when the particle reaches a detector, located at a known distance from the point where the reaction is taking place. This time interval is related to the particle energy. The time taken for a 1 Mev neutron to travel a distance of 1 meter is about 70 nsec., which is typical of the time intervals measured in fast neutron time-of-flight spectra. Time intervals are measured by means of a time-to-amplitude converter, which provides voltage pulses whose amplitudes are proportional to the corresponding time intervals. The resolving time of the entire system determines the neutron energy resolution obtainable with a flight path of given length. To obtain adequate separation of the neutron groups in typical fast neutron time-of-flight spectra requires a resolving

time of the order of a few nsec or less.

1.1.2. A d.c. beam system

A nuclear reaction is characterized by an associated γ-ray or a nuclear recoil, or both. When a target is bombarded by a beam from an electrostatic or cascade accelerator, the associated γ-ray or nuclear recoil, could be used to define the zero time for neutron time-of-flight experiments. In this case the zero time is produced by a scintillator attached to a photomultiplier, mounted a short distance from the target. The output pulses from this photomultiplier, after proper amplification and shaping, are fed into the time-to-amplitude converter. Neutrons are detected by a neutron scintillator and a fast photomultiplier. The resulting pulses are fed, after amplification and shaping, into the second input of the time-to-amplitude converter.

To obtain a zero time pulse from a recoiling nucleus, requires that it penetrates part of the target to reach the detector. Because of the very low penetrating power of low energy recoiling nuclei, this method is seldom used and will not be considered further.

In the case where the γ-ray is employed to produce the zero time pulse, only prompt γ-rays are

of use. In some nuclei the finite life time of the excited states will result in an uncertainty in the zero time, for example, the first excited state of B^{10} has a life time of the order of 1 nsec.

When an accelerated d.c. beam bombards a target, the pulses in the zero timing channel are random, resulting from the prompt γ-rays, and a certain amount of γ-ray background. Thus in addition to the real ones, many of the time-to-amplitude converter output pulses, will be due to random coincidences between background or prompt γ-rays, and neutrons. A second source of a background in the spectrum, is due to the sensitivity of the neutron detector to γ-radiation. Some types of fast neutron detectors, for example a liquid scintillation counter, produce pulses whose shape depends upon whether a neutron or γ-ray was detected. A special type of discriminator, called a pulse shape discriminator, can be used to eliminate any γ-ray or other noise pulses from the neutron channel. Most of the γ-ray detectors and photomultipliers used for the zero timing channel have output pulses with rise-time between 5 to 10 nsec. This will limit the resolving time of the entire system, unless a complicated electronic design is employed. (For more details see Chapter 5).

1.1.3. A pulsed beam system

A more recent development, which overcomes many of the difficulties of the d.c. system, utilizes pulses of beam produced by the accelerator. Zero timing pulses are produced by a purely electronic system, which detects the arrival of pulses of beam at the target. The zero timing channel in this case consists of standard pulses with a constant repetition rate depending only on the nature of the beam. Thus the random background in the time-of-flight spectrum is reduced to a minimum and the peak current in the pulse could be increased to its maximum value, so reducing the time of experiment by a large factor as compared with the d.c. beam method. The neutron counting channel is identical in both cases. A γ-ray pulse shape discriminator could be added although it does not play such an important role as in the first method. The spectrum obtained by the d.c. beam method, when utilizing γ-rays to produce zero timing pulses, does not include the neutron group corresponding to the formation of the product nucleus in the ground state, as there are no associated γ-rays in this case. Assuming the resolving time of the electronic system to be short enough, the resolving time in a spectrum, obtained with a pulsed beam, depends in most cases

entirely on the duration of the bursts.

It seems to be that the only advantage of the d.c. system is that, by selecting n-γ coincidences with only one known energy of γ-ray, it is possible to obtain any required section of the neutron time-of-flight spectrum, by choosing the appropriate γ-ray energy. Furthermore, selecting only one range of the neutron energy will allow the investigation of the associated γ-rays.

The aim of the research is to modify the 1.2 Mev. Philips High Voltage Generator, so as to produce either the usual d.c. beam, or a pulsed beam, with a pulse-duration in the region of nanoseconds, in order to make possible neutron time-of-flight experiments.

1.2. General Review

1.2.1. Means of production of bursts

There are two means of producing bursts of ions from an electrostatic or cascade generator, in the nsec region. These are: (a) beam chopping, (b) bunching. The first method is most commonly employed. The chopping of a beam can be achieved by passing it between a pair of deflector plates, fed with a variable voltage, and so sweeping the beam across an aperture[1], located at a certain distance from the deflector plates. To obtain

bursts with a duration of the order of a few nsec., the length of the deflector plates should be of the order of a few cm., when the deflected beam energy is a few keV, and ten times longer when the beam energy is of the order of a few Mev (for details see Chapter 3).

Bunching consists of the changing, in a time correlated fashion, of the energy or momentum of bursts of ions, in such a manner that the trailing ions of a burst will overtake the leading ions at a specific distance or time. This could be done by (a) increasing the energy of the trailing ions so that after a prescribed time they will catch up with the leading ions; or (b) causing the leading ions to travel a longer path so that they will meet the trailing ions at a certain point. Method (a) is the common klystron bunching used with electrons[2]. Method (b) has been proposed by Mobley[3] and is the more commonly used with protons or deuterons. The klystron principle utilizes the idea of passing ions through a gap, with a variable potential across it, in such a way that the first ions to arrive at the gap will gain less energy compared with the later ones. Calculations show that this system, applied to a 1 Mev proton beam, would require a drift distance[4] of the order of 8 meters. Therefore this is not

practicable for most electrostatic or cascade generators. Mobley has suggested a bunching magnet with a magnetic field distribution such that, if the beam is swept across one of the pole faces, the leading ions will arrive at a certain point at the same time as the trailing ones. Details of this system are given in Chapter 8. It is shown that the magnet radius should be of the order of 30 cm. for 1 Mev ions.

As clearly defined pulses could not be obtained by the bunching system alone it is usually used only as a second stage to reduce the time of bursts obtained by chopping.

1.2.2. Post acceleration and terminal pulsing

The pulsing of a d.c. beam, could be either a post-acceleration pulsing[5], or a terminal pulsing.[6,7,8,1] In the post-acceleration pulsing method the beam is pulsed between the accelerator and target, there being no need to change the accelerator itself. The advantages of this system are its simplicity, and the possibility of getting shorter pulses, for reasons which will be discussed later. The disadvantage is that only a small fraction of the total current is used, while the remainder produces an undesirable background. This creates a difficult shielding problem, between the pulsing section and

the target. The target must be moved a considerable distance, of the order of 4 meters[5], from its original position, so that the deflecting system, the shielding and an extra focussing lens can be accommodated. In the case of a cascade generator such as ours, the beam will have a very large diameter when it reaches the target unless a strong focussing lens is inserted between the pulsing system and the target.

In terminal pulsing, bursts of ions are produced after the ion source and before the main acceleration electrodes. In this case space limitation within the terminal has to be taken into consideration. In our particular case, the high voltage terminal is so close to the ceiling that any enlargement of the terminal might well cause sparking between the terminal and the ceiling, at the higher voltages. Another problem lies in the difficulty of providing extra electrical power for the pulsing equipment within the terminal. Another point which must be considered is that bursts obtained by terminal pulsing are slightly longer than those obtained by a post-acceleration system, because of the energy spread of the ions as a result of the pulsing. On the other hand, terminal pulsing eliminates most of the γ-ray and neutron background, which is due mainly to the beam hitting

metallic surfaces around the target. Because of the low mean d.c. current through the accelerator itself, it is possible to increase the current during bursts without having excessive X-ray and electron loading on the machine.

To avoid many of the disadvantages of these two systems, when a very large peak current with a very short burst duration is required, a system which employs terminal pulsing with bunching after acceleration, by a bunching magnet, was developed.(9,10) Bursts with a duration of less than one nanosecond and a peak current of a few milliampereswere obtained. This system is far more expensive and complicated than the others, but terminal pulsing only, which has great advantages over post-acceleration pulsing, could be built as a first stage, so that a bunching magnet could be designed and used if necessary at a later time.

In view of these considerations it was decided to build the terminal pulsing system, and to add a bunching magnet later on if desired.

2. DESCRIPTION OF THE PHILIPS 1.2 Mev CASCADE GENERATOR

The accelerator consists of two sections, the high voltage generator and the acceleration column.

The generator is a six stage multiplier, operating on the voltage-doubler principle. A motor generator with a regulated output voltage of 0 to 250 volts 200 Hz, feeds a 120 kvolt high tension transformer. The mercury rectifiers of the multiplier are fed by this transformer. The high voltage is adjusted between 250 and 1200 kvolt, by adjusting the motor generator output voltage. The condensers of the voltage multiplier have capacities of 0.018 μF. To limit charging currents, each of the mercury rectifiers has a series wire wound resistor of approximately 50,000 ohms. The heating of the rectifiers' cathodes is accomplished by current from a 0.5 MHz oscillator. A 200 megohm carbon film resistance, cooled by circulating oil, is connected between the high voltage terminal and ground. The current through this resistor is the measure of the high voltage.

The acceleration tube is built of six ceramic insulators whose ends are ground flat so that they fit to round steel plates, which hold five acceleration electrodes. Gaskets, between the ground surfaces of the ceramics and the steel

plates, keep the joints vacuum tight. The acceleration electrodes are connected to the different stages of the voltage multiplier. The acceleration column is evacuated by a combination of rotary and oil diffusion pumps, to a pressure of less than 10^{-5} mm. The top section of the acceleration column is shown in Fig. 1. This consists of the top ceramic insulator, an ion source supplying ions to the acceleration column, a focussing lens, for focussing of the ion beam, and the first acceleration electrode. The ion source consists of a radio frequency gas discharge, from which an ion current of up to 500 μA can be extracted through a canal in an aluminium electrode. A.K. Ganguly and H. Bakhru have described in detail[11] this type of ion source, and discussed ways of obtaining maximum current. Current extracted from an ion source depends on various parameters, including:

(1) the extraction probe voltage,

(2) the plasma density, which in turn depends on
   (a) the r.f. power,
   (b) the gas pressure,
   (c) the magnetic field, and

(3) the canal geometry.

The extraction current increases as the probe voltage is increased and reaches some saturation value which depends on the r.f. oscillator power. The maximum current is also a function of the gas pressure. It increases with

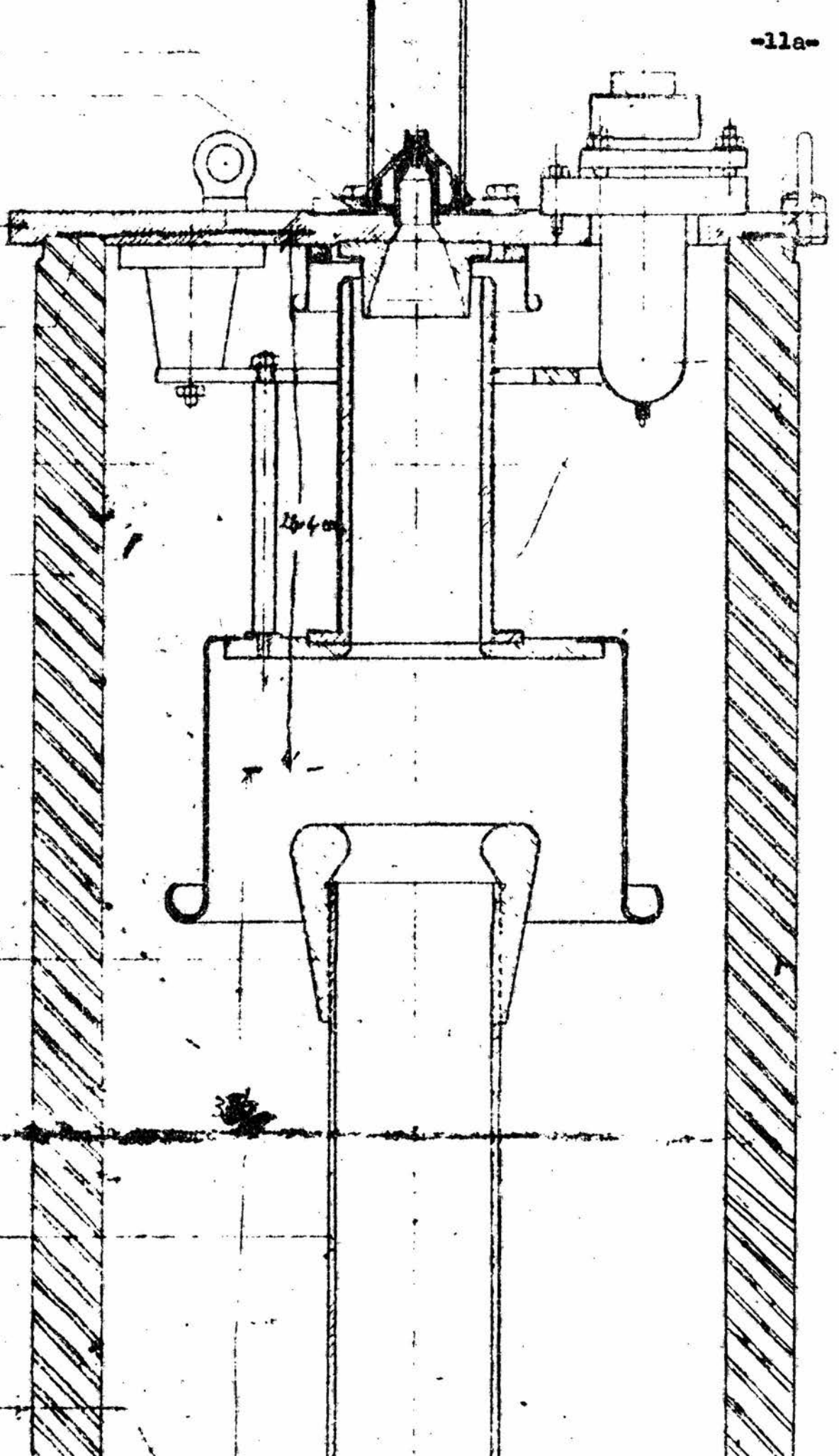

Fig. 1 TOP SECTION OF ACCELERATION COLUMN

gas pressure, passes through a maximum and then falls. Thus for each oscillator power there is an optimum pressure at which the current is a maximum. There is an optimum axial magnetic field for which the extracted current will reach its maximum value. This is mainly dependent on the probe voltage. The current is also dependent on the canal geometry. Its value increases as the square of the canal diameter (d), and is inversely proportional to the square value of the canal's length (ℓ).

The extraction current I, before reaching saturation, is

$$I \propto U^{3/2}\left(\frac{d}{\ell}\right)^2 \qquad (1)$$

where U is the probe voltage.

The maximum canal diameter is limited by the maximum pressure allowed around the terminal electrodes (conductance varies as d^3/ℓ), and therefore by the pumping speed of the diffusion pump, connected to the system. Too large a pressure will cause scattering and neutralization of the ion beam, which will be particularly noticeable when trying to obtain large currents. In some cases an extra diffusion pump has been connected just below the aluminium canal to reduce the effect of gas flow through the canal. In our case

there is no extra pump for this purpose, and the canal diameter is limited to about 1.2 mm. Control of the ion current from the source is obtained by varying the extraction potential U, its maximum value being given by the insulating properties of the ion source envelope. In the case of the ion source fitted to the cascade generator, this voltage is adjustable between 0 and 5 kvolt. The higher the power supplied by the exciting oscillator, the higher the current available from the ion source. In our case the r.f. oscillator is a conventional 40 MHz oscillator with an output power of about 100 watts. The tank coil consists of 6 turns of copper tube, surrounding the glass envelope of the ion source. Two permanent magnets, one on each side of the ion source envelope, just above the level of the canal, provide a predominantly axial focussing magnetic field, which increases the extracted ion current.

The ions, after extraction through the canal, are first focussed by an electrostatic lens and then accelerated. The focussing electrode (Fig. 1) is a steel cylinder, 5 cm. diameter and 20 cm. long, supplied with an adjustable negative voltage of between 0 and 50 kvolt. The lower edge of the same cylinder is used for focussing the beam of the whole generator. Fig. 2 is a block diagram of

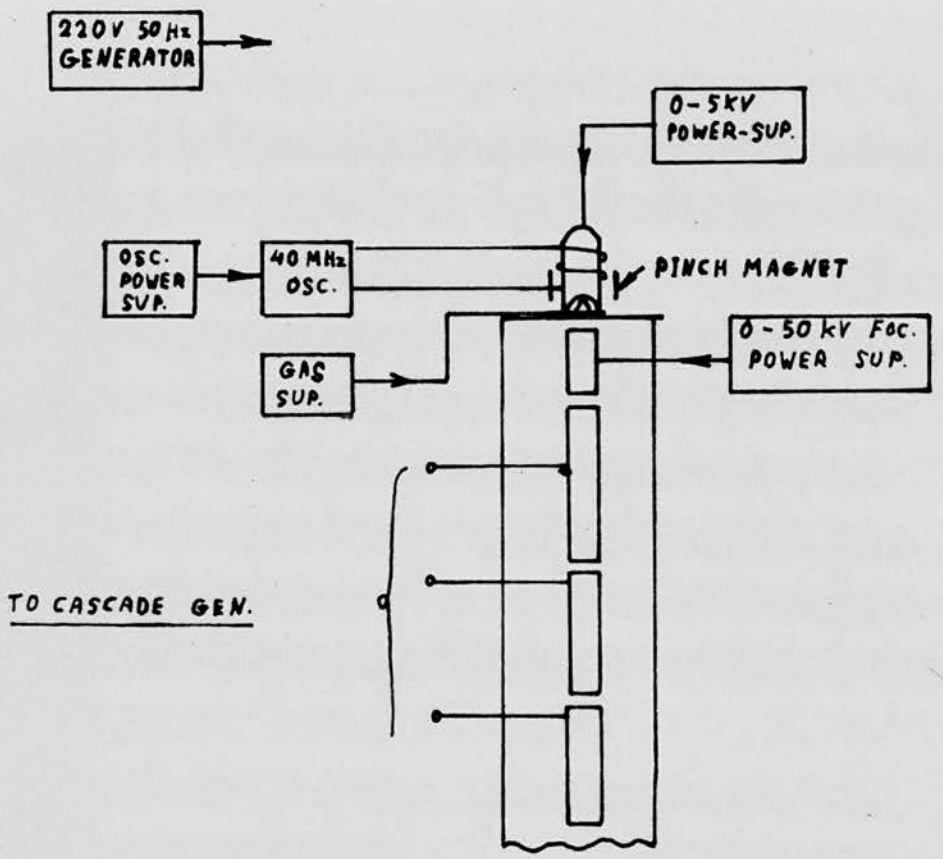

Fig. 2 BLOCK DIAGRAM OF THE TERMINAL

the equipment in the high voltage terminal. The power for the electronic equipment at the high voltage terminal is supplied by a 50 Hz, 220V, 2KW generator. The generator is driven, by means of an isolating belt, by a motor located at the bottom of the acceleration column.

The ion beam is accelerated by the voltage supplied to five cylinders of the same diameter. The first one is about 80 cm. long, while the other four are each about 55 cm. long. The gap between adjacent electrodes is about 5 cm. Successive accelerating electrodes are connected to successive stages of the cascade generator, so that the potential difference across each gap between neighbouring electrodes is the same. Fig. 3 shows the change of the ion energy E, as the beam approaches the target. The main focussing of the beam is done between the focussing and the first acceleration electrodes, where the ion energy is relatively low. It can be shown that a second focussing occurs in the gap between the first and second acceleration electrode. The other acceleration electrodes do not have much focussing effect, but they keep the beam in shape until it reaches the target. The main reason for having a number of electrodes is to eliminate discharges on the insulators by obtaining a uniform electrostatic

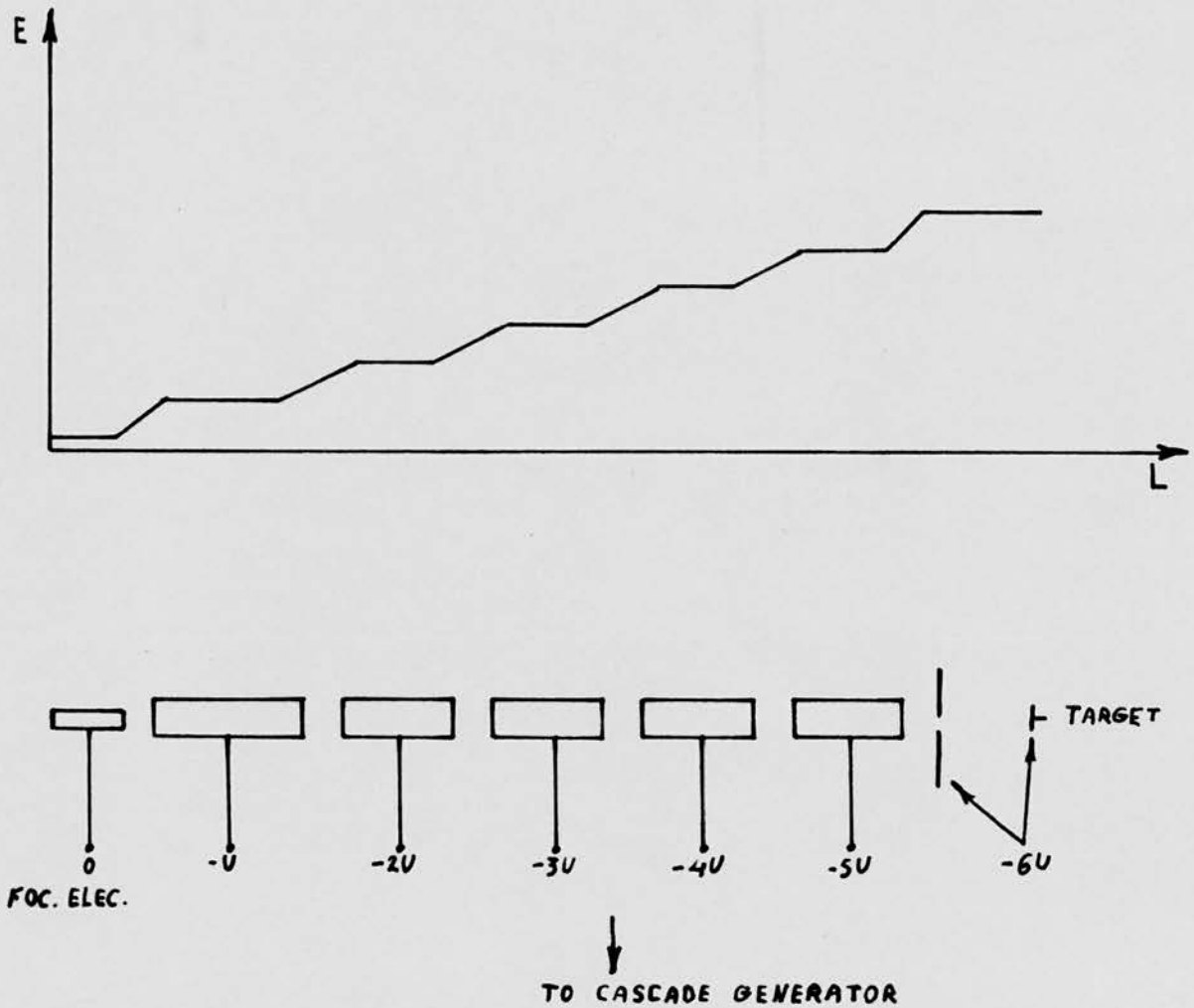

Fig. 3 VOLTAGES AND ENERGIES OF ELECTRODS AND BEAM PARTICLES

field across the column.

The focussing properties of the entire system are discussed in more detail in the next chapter.

The current delivered to the target is about 500 μA in a region of about 10 millimeters diameter. The target is about 4 meters from the canal.

3. THE EXPERIMENTAL PULSED SYSTEM

3.1. General

As mentioned in the introduction, it is desirable not to extend the physical dimensions of the top of the accelerating column and therefore a new and shorter focussing system had to be designed. The first larger acceleration electrode was changed to a shorter one, identical to the others. A new lens was designed so as to focus the beam from the canal to an image point in the region of the pulse section, (Fig. 4). A second focussing between the pulse section and the near first acceleration electrode would achieve a sharp beam image on the target. The shortening of the first electrode and the use of a new focussing lens extends the available space within the existing acceleration column.

Since experiments required the accelerator, it was necessary to try an experimental system first, consisting of an ion source and pulse system. Fig. 5 is a photograph of the final experimental system. It was built inside a ceramic cylinder maintained at high vacuum by rotary and diffusion pumps. The pumps and a target were connected to the bottom flange (Fig. 6), while the ion source section was mounted on top.

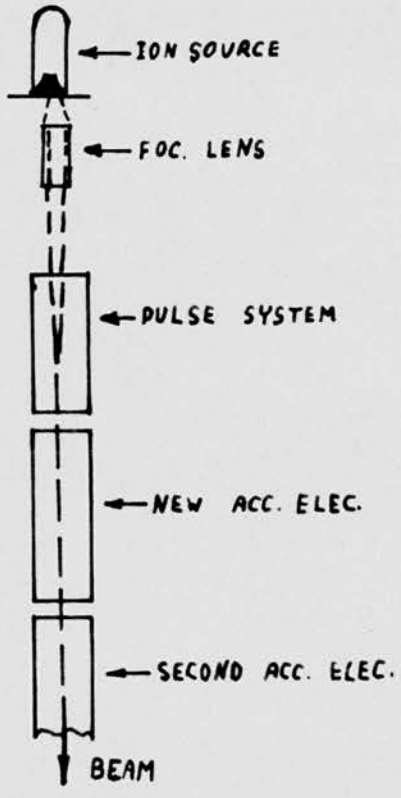

Fig. 4 ARRANGMENT OF THE NEW TERMINAL

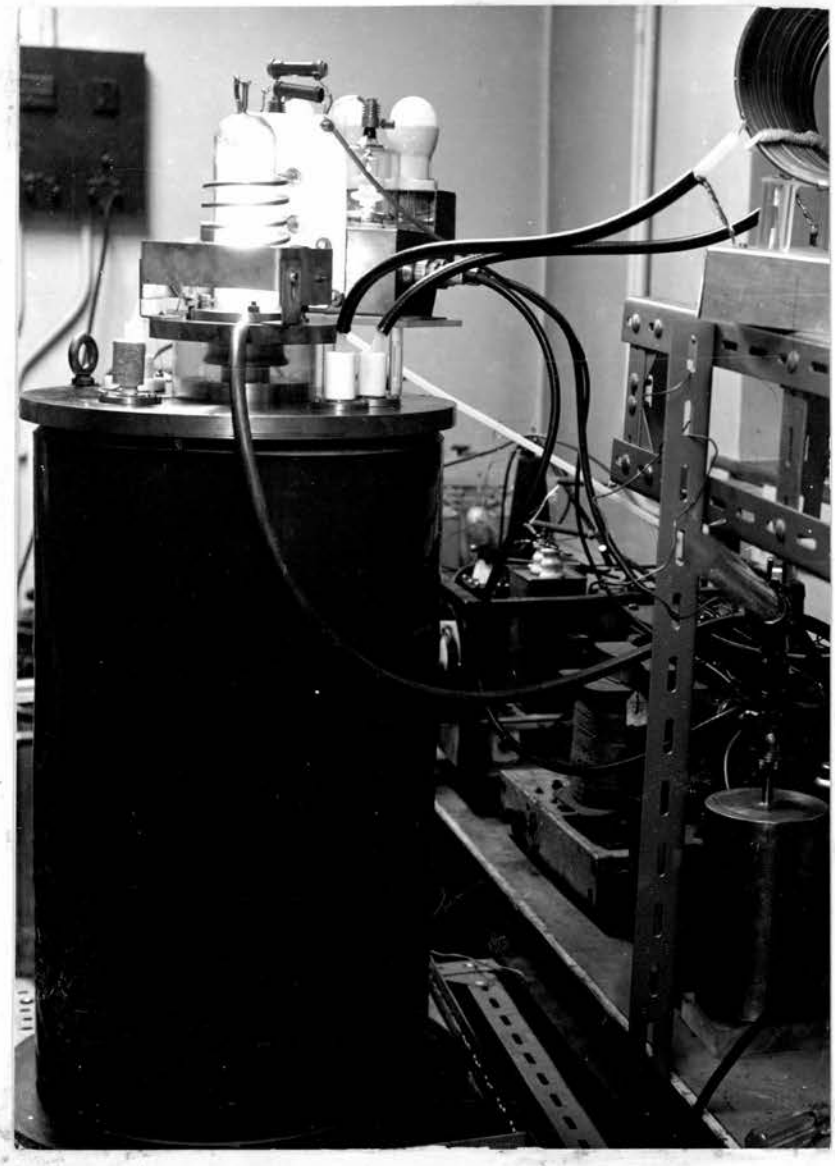

FIG. 5. The Experimental System

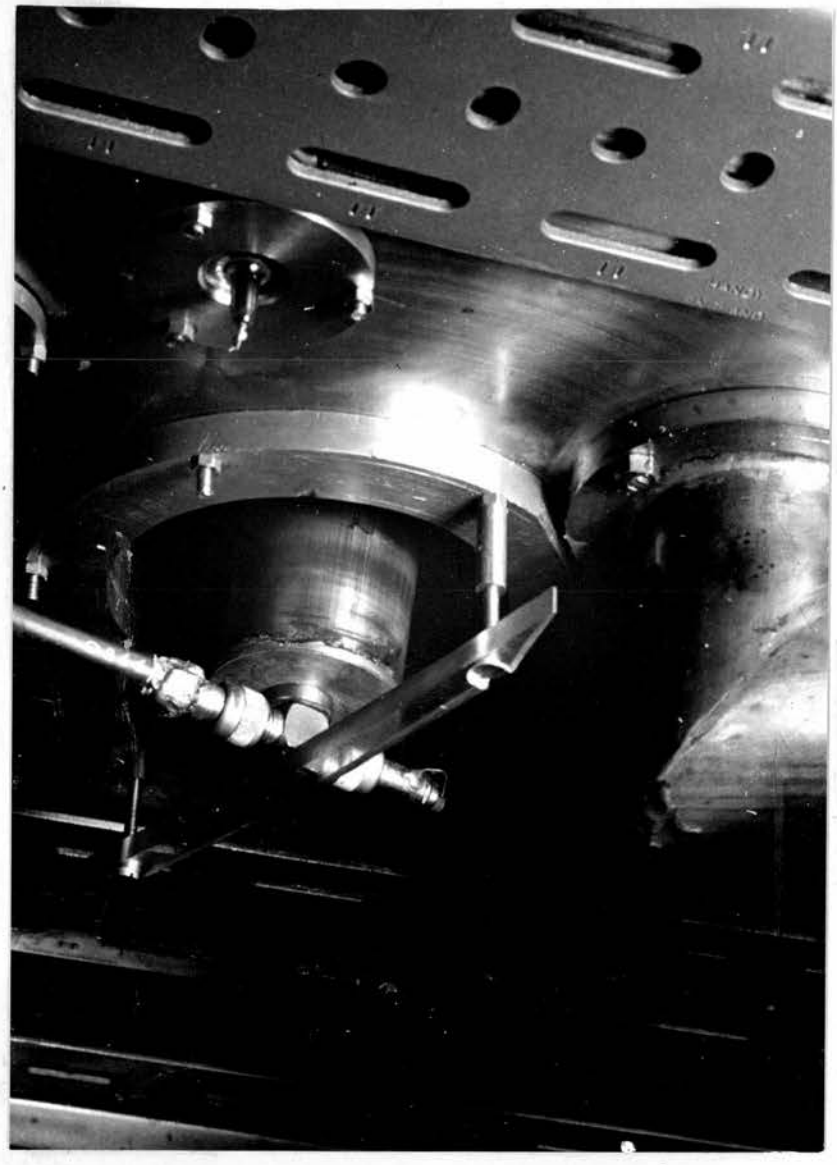

FIG. 6 Arrangement of Target and Pump in The Experimental System.

3.2. The Ion Source section

For reasons which will be explained later the ion source assembly has to be electrically isolated from the other sections. This was done by putting the ion source on a flange isolated by a glass cylinder (Fig. 5 and Fig. 7). An isolated oscillator, of the same type as that in the main set, was used and with a 5 kV probe power supply. Fig. 7 shows the block diagram of the ion source system. The isolation is effected by a 1:1 1 kwatt, 30 kV, isolation transformer, specially designed by Ferranti. The gas supply is isolated by connecting a glass tube, about 15 cm. long, between it and the ion source (Fig. 7). This ion source should have a performance identical to that of the ion source operating in conjunction with the main set.

3.3. The focussing system

In order to get a well focussed beam on the target of the main accelerator, the ions entering the first acceleration electrodes should have a pre-acceleration energy with a minimum spread. The optimum pre-acceleration energy is about 15 keV, depending on the accelerator voltage. The energy of the ions when extracted through the aluminium canal is almost the same as the probe voltage with

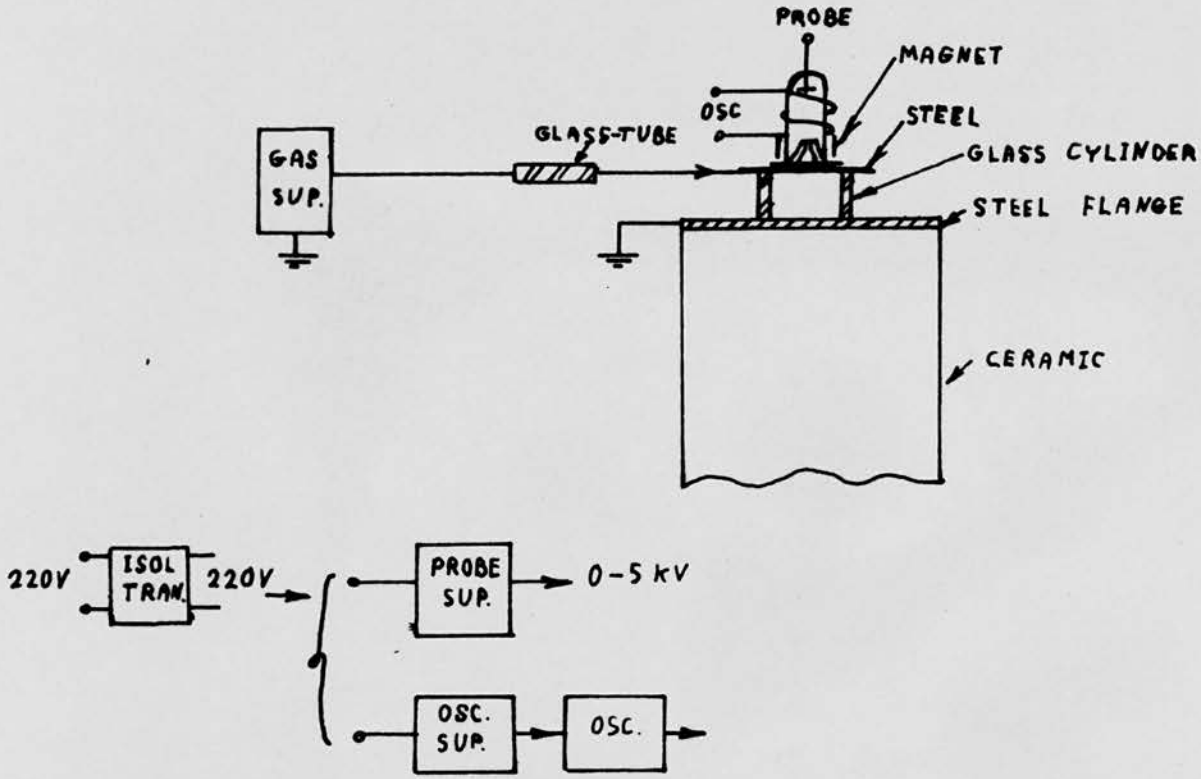

Fig. 7 ION SOURCE ASSEMBLY

a small spread. In a pulsed machine where maximum currents are usually required, this voltage is about 4 kV. To reach the desired pre-acceleration energy the first section of the focussing lens is designed to act as a pre-acceleration electrode. An Einzel type lens is used, composed of three sections (Fig. 8). These are stainless steel cylinders with the same internal diameter of 35 mm. The first cylinder is 10 cm. long with an aperture of 6 mm. diameter at the top. The second is 2.5 cm. long fixed 4 mm. below the top cylinder. The third is 8 cm. long fixed 4 mm. below. Stainless steel flanges are welded to each of the cylinders (Fig. 13). Four quartz rods, joined by Araldite, separate the three sections, keeping them in good alignment even with changes in temperature. The top and bottom sections have the same potential (zero potential) and the centre section has a potential about equal to the pre-acceleration potential. As the top section of the Einzel lens is at a zero potential the ion source is held at a potential of up to + 20 kV. This requires that the ion source assembly be insulated from the rest of the system. Ions extracted by the canal are accelerated to a higher energy, by the aperture of the Einzel lens which is 10 mm. below the canal. The top section of the Einsel lens is long enough

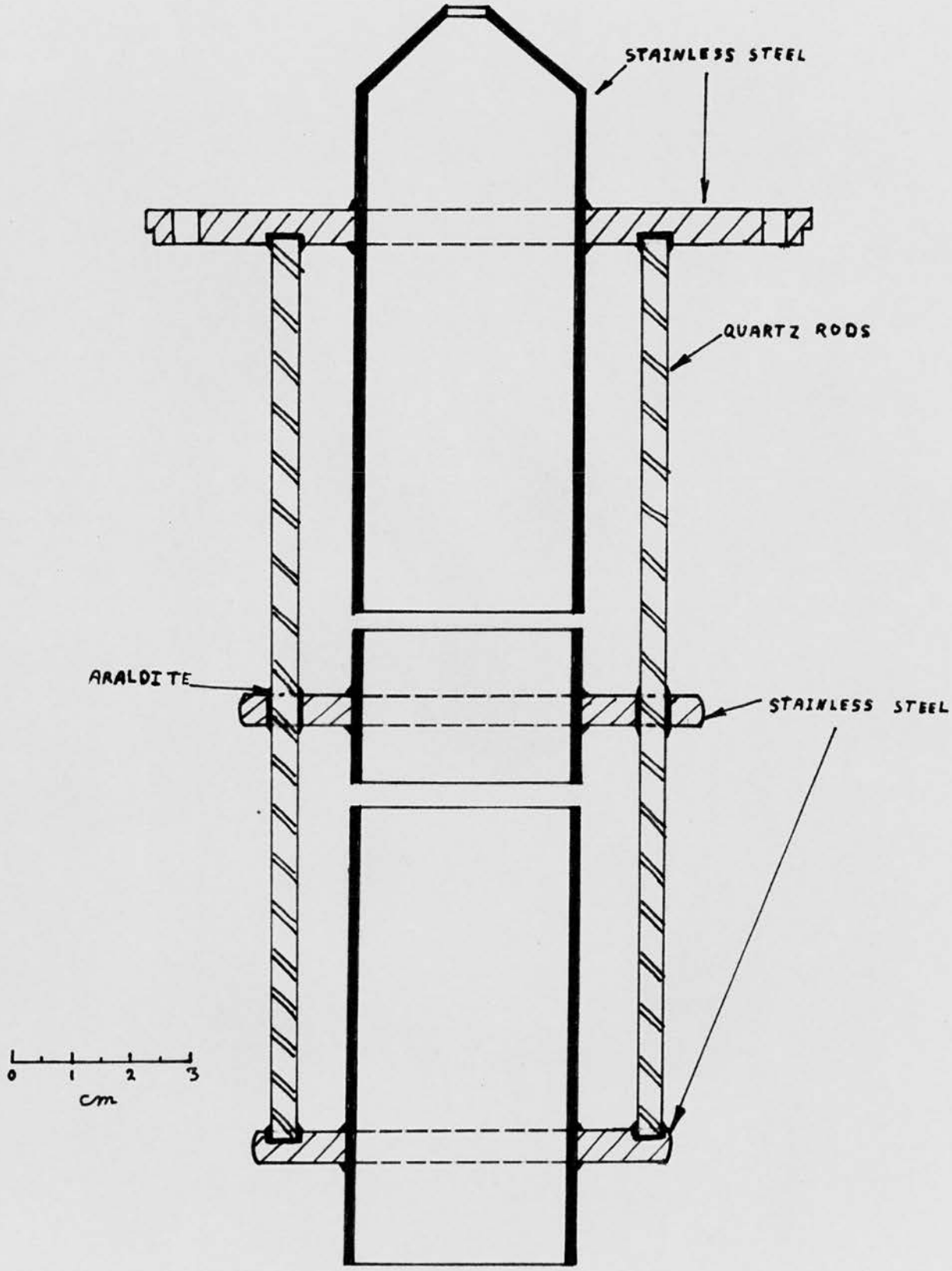

Fig. 8 THE EINZEL LENS.

so that the ions will have the pre-acceleration energy before reaching the lower edge of the electrode and they will form a parallel axial beam. There are two focussing fields in this lens, one between the two centre sections and the other between the centre and bottom sections. The first is decelerating and the second accelerating field. Thus ions leaving the focussing Einzel lens will still have the same pre-acceleration energy.

The focussing is calculated by means of Maxwell's equation

$$\text{div } E = \frac{\rho}{\varepsilon} \qquad (2)$$

where E = electrostatic field

ρ = charge density

ε = dielectric constant

in cylindrical coordinates this equation will be of the form:

$$\frac{1}{r}\frac{\partial}{\partial r}(rEr) + \frac{1}{r}\frac{\partial E\theta}{\partial \theta} + \frac{\partial Ez}{\partial z} = \frac{\rho}{\varepsilon} \qquad (3)$$

In an electrostatic field

$$E_r = -\frac{\partial U}{\partial r}$$

$$E_\theta = -\frac{1}{r}\frac{\partial U}{\partial \theta} \qquad (4)$$

$$E_z = -\frac{\partial U}{\partial z}$$

The equation of motion in an electrostatic field is given by

$$\frac{d}{dt}(mv) = eE \qquad (5)$$

where m = mass of particles

v = velocity of particles.

In cylindrical coordinates

$$\frac{d}{dt}(mr) - mr\dot{\theta}^2 = eE_r$$

$$\frac{1}{r}\frac{d}{dt}(mr^2\dot{\theta}) = eE_\theta \qquad (6)$$

$$\frac{d}{dt}(m\dot{z}) = eE_z$$

The potential distribution along the z axis is represented by

$$U(r = 0) = U_o(z) \qquad (7)$$

It is assumed that this potential is referred to zero at a point where the particle energy is zero, so that U is a measure of particle energy.

To satisfy Laplace's equation we can write

$$U = U_o - \frac{r^2}{4}\frac{d^2U_o}{dz^2} + \frac{r^4}{64}\frac{d^4U_o}{dz^4} \cdots \qquad (8)$$

For most lens systems it is necessary to retain only the first two terms, so we shall use

$$E_z = -\frac{dU_o}{dz}$$
$$E_r = \frac{r}{2}\frac{d^2U_o}{dz^2} \qquad (9)$$

The radial equation of motion ($m\ddot{r} = eE_r$) will have the form

$$m\ddot{z}\frac{dr}{dz} + m\dot{z}^2\frac{d^2r}{dz^2} = eE_r \qquad (10)$$

But $m\ddot{z} = eE_z = -e\frac{dU_o}{dz}$ and $m\dot{z}^2 = 2eV$

so that

$$Ur'' + \frac{U'r'}{2} + \frac{U''r}{4} = 0 \qquad (11)$$

This equation is known as the "ray equation".

In the case of focussing between the ends of two coaxial cylinders (Fig. 9) it can be shown[12] that there is very little difference between the focussing effect of an accelerating field and that of the decelerating one. Results obtained by means of the above equation are given in Fig. 10[12]. These do not take into consideration the space charge, existing when focussing a higher intensity beam, causing abberation. In addition the diameter of the beam is assumed to be a small fraction of the cylinder diameter.

The Einzel lens is a symmetrical lens and the potential is the same on the two sides of the system. The form of the field in the Einzel lens is shown in Fig. 11. This lens will always be converging no matter whether the central electrode is positive or negative with reference to the other two.

The field in the centre can be evaluated from a particular solution of Laplace's equation[13]

$$V_{zr} = \frac{1}{2\pi} \int_0^{2\pi} f(z + ir \sin \alpha)\, d\alpha \qquad (12)$$

The limiting equipotentials which cross at the centre of the lens make an angle of $54^\circ\ 44'$ with the axis. This angle is independent of the shape of the electrodes. The lens is called an Einzel

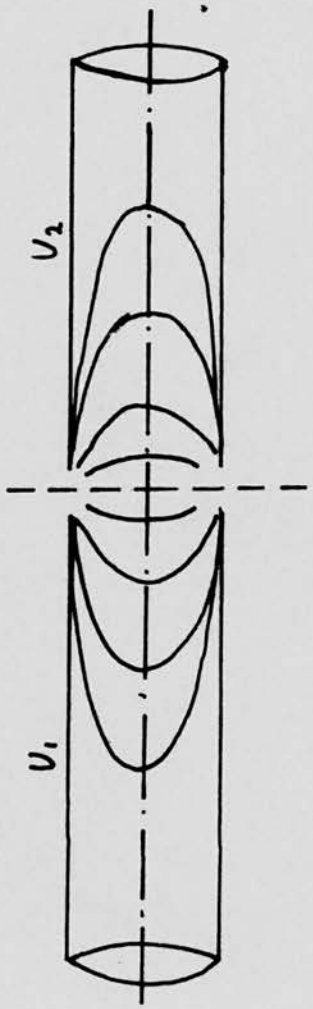

Fig. 9 FOCUSSING FIELD BETWEEN TWO CYLINDERS.

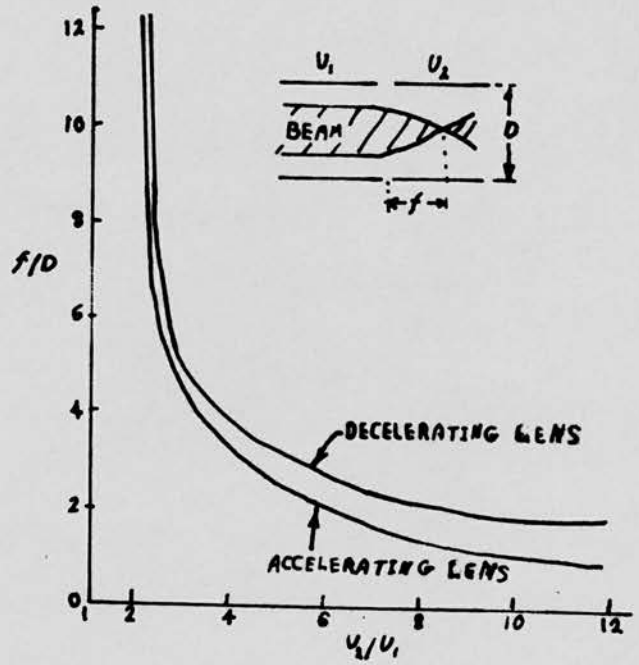

Fig. 10 FOCAL LENGTH FOR DOUBLE CYLINDER LENSES

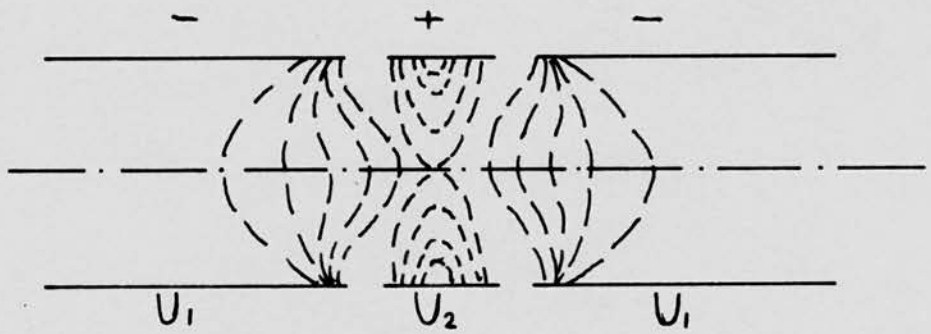

Fig. 11. EQUIPOTENTIAL LINES IN THE EINZEL LENS

lens because it has the same shape of field as an isolated aperture when the gradient is of opposite sign on the two sides.

From equation (11) we get

$$- V'' r/4 = V'r'/2 + Vr'' = V \frac{d}{dz}(r' \sqrt{V}) \qquad (13)$$

Integration gives

$$\left| r' \sqrt{V} \right|_a^z = - \frac{1}{4} \int_a^z \frac{rV''}{\sqrt{V}} \, dz \qquad (14)$$

Having a particle enter the system parallel to the z axis at z = a, we get

$$\left(\frac{dr}{dz} \right)_a = r'_a = 0 \qquad (15)$$

Hence

$$r'_z = -\frac{1}{4\sqrt{V}} \int_a^z \frac{rV''}{\sqrt{V}} \, dz \qquad (16)$$

This last equation could only be solved by successive approximation.

If $r' = r_o' + r_1' + r_2' + \cdots\cdots$

where $r'_o = r'_a = 0$ and $r_o = r_a$

then

$$r_1' = - \frac{1}{4\sqrt{V}} \int_a^z \frac{r_o V''}{\sqrt{V}} \, dz$$

$$= - \frac{r_a}{4\sqrt{V}} \int_{-\infty}^z \frac{V''}{\sqrt{V}} \, dz \qquad (17)$$

and $$r_1 = - \frac{r_a}{4} \int_{-\infty}^z \frac{1}{\sqrt{V}} \int_{-\infty}^z \frac{V''}{\sqrt{V}} \, dz \, dz \qquad (18)$$

in the same way we get

$$r'_b = r_a \left[\frac{1}{4\sqrt{V_b}} \int_{-\infty}^{z_b} \frac{V''}{\sqrt{V}}\, dz + \frac{1}{16\sqrt{V_b}} \int_{-\infty}^{z_b} \frac{V''}{\sqrt{V}} \int_{-\infty}^{z} \frac{1}{\sqrt{V_b}} \int_{-\infty}^{z} \frac{V''}{\sqrt{V}}\, dz\, dz\, dz \right.$$

$$\left. \cdots\cdots \right] \qquad (20)$$

r'_b is the total deviation of the beam produced by the lens and V_b is the potential of the image space. It could be shown[13] that

$$\frac{1}{f_2} = -r'_b/r_a =$$

$$= \frac{1}{4\sqrt{V_b}} \int_{-\infty}^{\infty} \frac{V''}{\sqrt{V}}\, dz - \frac{1}{16\sqrt{V_b}} \int_{-\infty}^{\infty} \frac{V''}{\sqrt{V}} \int_{-\infty}^{z} \frac{1}{\sqrt{V_b}} \int_{-\infty}^{z} \frac{V''}{\sqrt{V}}\, dz\, dz\, dz$$

$$+ \frac{1}{4^3\sqrt{V_b}} \int_{-\infty}^{\infty} \frac{V''}{\sqrt{V}} \int_{-\infty}^{z} \frac{1}{\sqrt{V_b}} \int_{-\infty}^{z} \frac{V''}{\sqrt{V}} \int_{-\infty}^{z} \frac{1}{\sqrt{V_b}} \int_{-\infty}^{z} \frac{V''}{\sqrt{V}}\, dz\, dz\, dz\, dz$$

$$\cdots\cdots\cdots \qquad (21)$$

Once the axial distribution of potential and its derivatives have been found, a numerical evaluation of the expression may be made. Johannson and Scherzer[13] plotted focal length (f) against the ratio $\frac{(U_2 - U_1)}{U_1}$ (Fig. 12). These results are true as long as the length of the second section is shorter than twice the diameter of the cylinder. A big advantage of this lens is that when the potential of the middle section U_2 is of about the same value as the energy of the particle at the source, the focal length will be

very stable and not dependent on fluctuation in the ion source energy.

It is assumed that the energy E_i, of ions inside the first and third cylinder, is equal to

$$E_i = U_a + U_p \qquad (22)$$

where U_a = preacceleration voltage,

U_p = probe voltage.

Entering the second cylinder, the ionswill lose some energy, reaching the energy E_f. To obtain minimum burst duration,the image should fall in the region of the pulsing system which is about 40 cm. from the aluminium canal. From Fig. 12 it can be seen that $\frac{E_f - E_i}{E_i}$ should have the value of 0.8.

Assuming a probe voltage of 5 kV and a pre-acceleration voltage of 13 kV, E_i is 18 kV, thus $E_f \approx 10$ kV. As all potentials are referred to the first cylinder (zero potential), the focussing voltage should be about 8 kV. To obtain the correct potentials, an auxiliary power supply of 0 to-5kV , connected in series with the pre-acceleration power supply, is connected to the centre cylinder.

The beam diameter was measured with different pre-acceleration voltages, and was found to be less than 1 mm. under the best of conditions. The

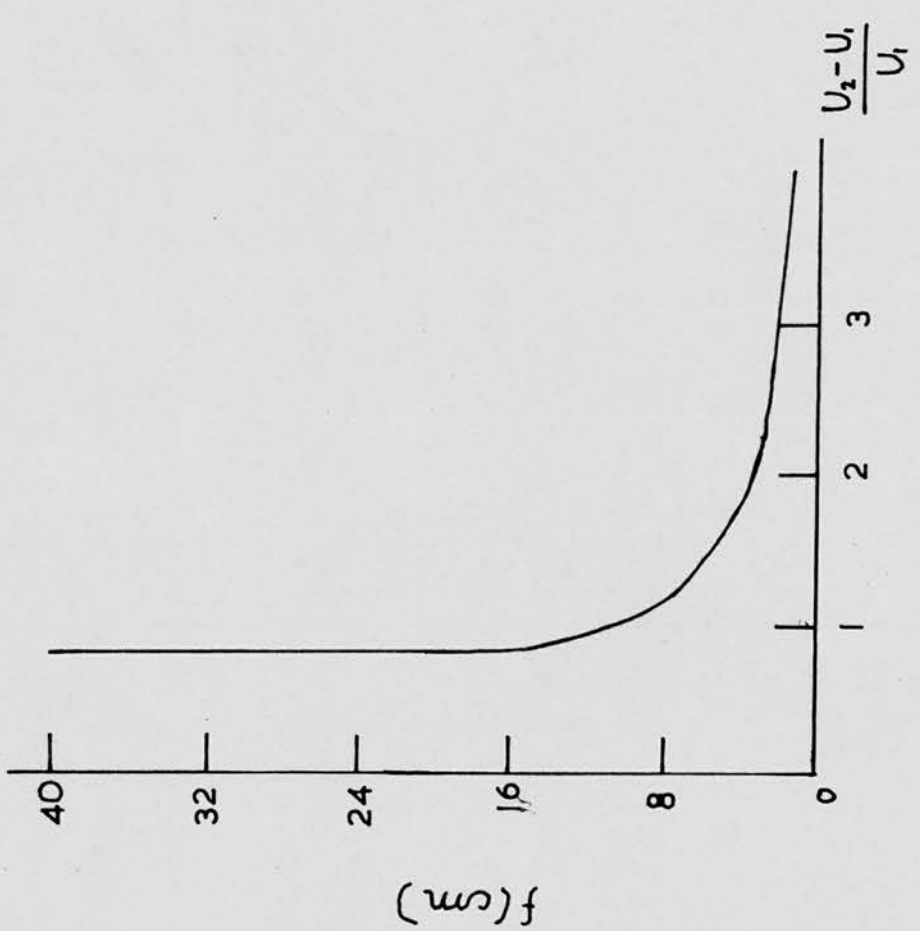

Fig. 12. FOCAL LENGTH OF THE EINZEL LENS.

diameter was measured by examining the discoloured area produced ~~performed~~ by the beam, on a steel target. There was no large abberation of focussing due to space charge, even with the maximum current available from the experimental system, a few hundred micro-amperes. A photograph of the Einzel lens is shown in Fig. 13.

3.4. The Pulsed Section

The principle of pulsing is based on ~~chopping~~ sweeping the ion beam, by a set of deflector plates, across an aperture. The beam is swept by the deflector plates, which are fed by a variable voltage and passes through the aperture. The sweeping voltage can be of two different forms,

a. Impulse sweeping,

b. Differential impulse sweeping.

In the first form, the d.c. steady beam is deflected from the axis, by a voltage pulse, causing it to pass through an aperture. In the case of no sweeping impulses no beam will pass through the aperture. Thus when a d.c. beam is required, a constant d.c. bias is needed on the deflector plates. The duration of the bursts is determined by the width of the sweeping pulse which should have a stable amplitude. A short duration voltage

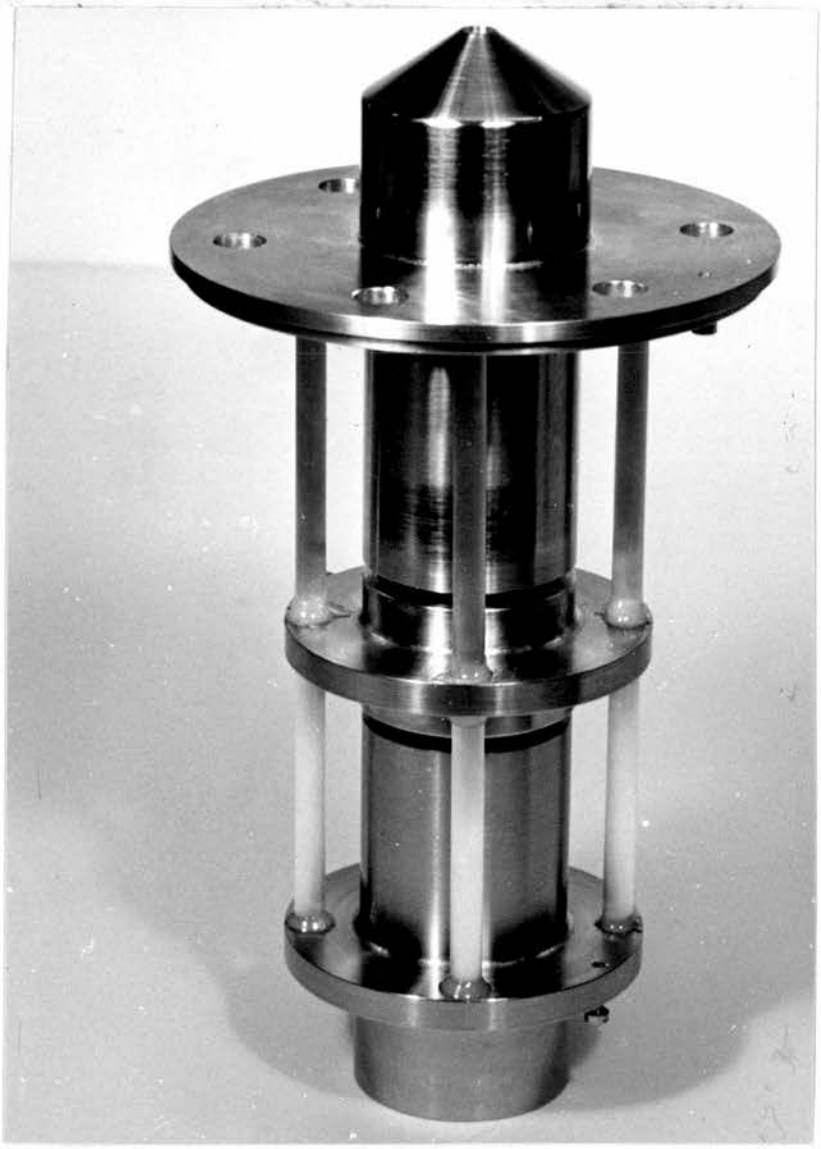

FIG. 13 The Einzel Lens

pulse with a stable high voltage amplitude is therefore required. These pulses are very difficult to produce and therefore the system is not practicable.

The second form consists of an alternating voltage feeding the deflector plates causing the beam to move from one side of the deflector plates to the other. If the period of the sweeping voltage is long compared with the time required for the beam particle to pass through the plates, only these particles which enter the deflector plates around the zero potential, will pass through the aperture. The last assumption requires an aperture coaxial with the deflector plates. The best sweeping voltage will be a saw-tooth generator. However, a sinewave voltage will give similar results if the amplitude is large enough. Thus the differential impulse sweeping voltage is usually a sinusoidal r.f. voltage with a frequency depending on the required repetition rate of the bursts of ions.

Fig. 14 shows schematically the two deflector plates and the aperture. For simplicity the space charge and fringing field effects are neglected.

If the beam enters the plates with velocity v_o, it can be shown[4] that the beam is deflected by an amount

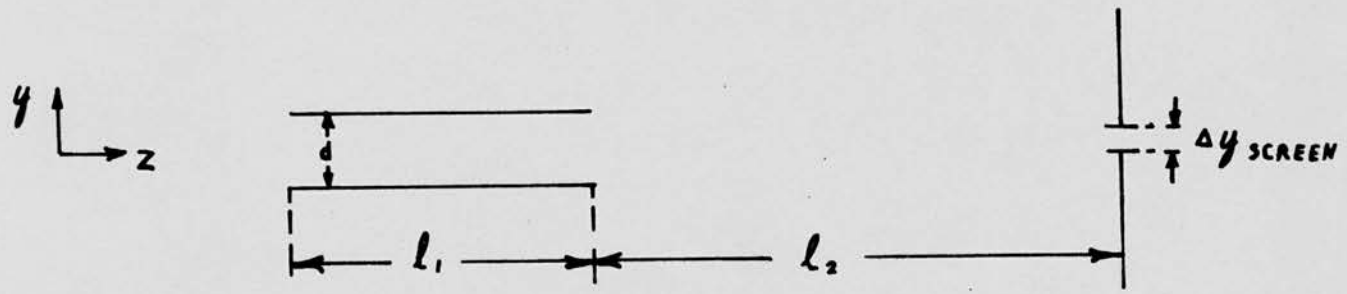

Fig. 14. SCHEMATIC OF DEFLECTOR PLATES AND APERTURE

$$\Delta y_{screen} = \frac{1}{4}\ell_1(\ell_1 + 2\ell_2)(eV_o/Ed)\Delta\phi \qquad (23)$$

where Δy_{screen} = deflection at the aperture

E = $\frac{1}{2}mv_o^2$

ϕ = ωt_o

e = charge of ions

V_o = Peak voltage supplied to deflector plates.

It follows that,

$$\Delta t_o = 4(Ed/\omega eV_o)\frac{\Delta y_{screen}}{\ell_1(\ell_1+2\ell_2)} = \frac{\Delta y}{w.s} \qquad (24)$$

taking Δy_{screen} as the aperture diameter, Δt_o is the burst duration. w.s. is the writing speed given by

$$w.s. = \omega e V_o \ell_1(\ell_1 + 2\ell_2)/4Ed \qquad (25)$$

This last result does not take into consideration the finite physical dimensions of the beam. It can be shown[4] that in the case of a beam having a diameter d_b the burst duration will be

$$\Delta t_o = 4(Ed/\omega eV_o)\frac{\Delta y_{screen} + d_b}{\ell_1(\ell_1+2\ell_2)} \qquad (26)$$

Because of the finite dimension of the beam entering the deflection system, some energy spread is introduced during the deflection process[14]. If the aperture is at a large distance from the deflector plates, the axial beam passing through

will enter and leave the deflector plates at approximately $-\frac{1}{2}\tau_1$ and $+\frac{1}{2}\tau_1$ respectively, with relation to the r.f. field. Looking at Fig. 15, an energy difference is observed between the beam rays 1, 2 and 1, 3

$$\Delta E = \frac{\ell_1 \Delta\theta}{d} \tau_1 feV_o \qquad (27)$$

This energy spread will cause a spread in the time taken by the ions to travel from the deflector plates to the aperture, and so defines a time limit to the possible burst duration. After passing through the aperture the ions enter the acceleration electrodes, and after a time T, of about 1 microsecond, reach the target. Assuming an energy spread ΔE within the ion burst, the corresponding time spread at the target will be

$$\Delta t = \frac{1}{2} T \frac{\Delta E}{E} \qquad (28)$$

where E is the total accelerating voltage expressed in energy units. Because of this time spread, pulses produced by a pre-acceleration system are longer than those produced by post-acceleration pulsing. This effect is more noticeable when pulsing a low voltage accelerator such as ours. When deuterons are accelerated to an energy of about 500 keV, the time T, required for the ions to reach the target (which is about 4 meters from

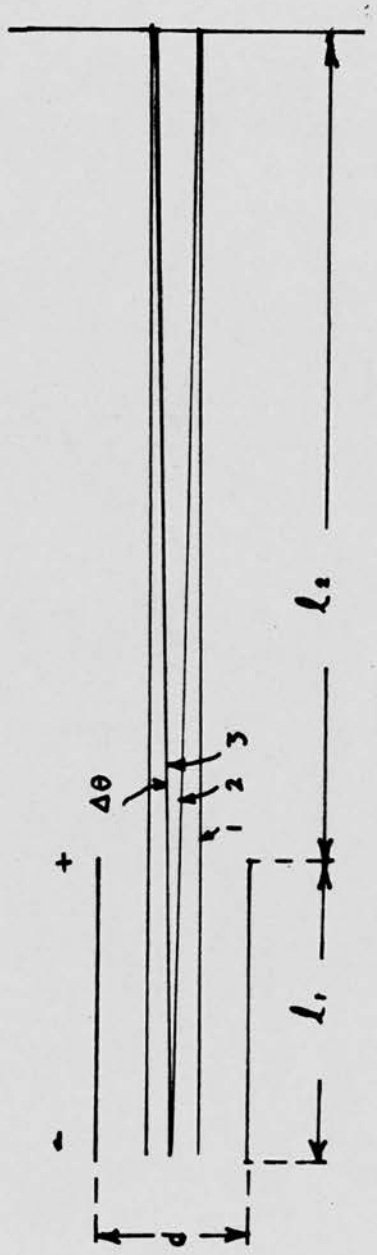

Fig. 15. ENERGY SPREAD IN DEFLECTOR PLATES

the source) is about 1 microsecond. Assuming an energy spread of about 1 keV, the corresponding time spread is 1 nsec. Thus pulses, having a duration of Δt after the aperture will have a longer duration at the target of Δt + 1 nsec. It can be shown[14] that the minimum burst duration available at the aperture is

$$\Delta t_{o_{min}} = \frac{\sqrt{\ell 2\, \Delta y_{screen}\, \Delta\theta}}{V_o} \qquad (29)$$

Thus increasing the pre-acceleration energy will reduce the burst duration, as will putting the aperture closer to the deflector plates. However making these changes requires a large increase in the deflection voltage. Reducing the aperture diameter will also reduce the burst duration without any necessary increase in the r.f. voltage. Δy_{screen} is usually determined by the size required to pass the d.c. beam.

When an r.f. sinusoidal field is applied to the deflector plates, whenever the r.f. voltage reaches zero potential a burst of ions passes through the aperture. Thus the burst repetition rate is twice the field frequency. Successive bursts will give two different images on the target. This is due to an upsweep field, first negative and then positive, which produces the first burst and

a downsweep field, first positive and then negative, which produces the second burst. It is sometimes advisable to eliminate one of these pulses. There are two ways of doing this. One involves another pair of deflector plates fed by an r.f. field, synchronized with the main field, but of an harmonic frequency. These are inserted between the first plates and the aperture and are rotated through 90° about the axis related to the main deflector plates. In this way the ions will have an elliptical track and only successive pulses will pass through the aperture.

The second method involves two extra pairs of deflection plates, supplied with a d.c. voltage with the polarity shown in Fig. 16. The two successive bursts are deflected in one direction so that only one of them will pass through the aperture, while the other will hit the refractor plates. This system has the advantage that the beam is deflected back towards the axis.

The entire pulsing system developed for our accelerator is shown in Fig. 17. The deflector plates are made of steel, 5 cm. long and 8 mm. apart. 1 cm. below are the steel refractor plates, each 2 cm. long and 8 mm. apart. Both deflector and refractor plates are supported by quartz insulators. 8 cm. from the deflector plates is

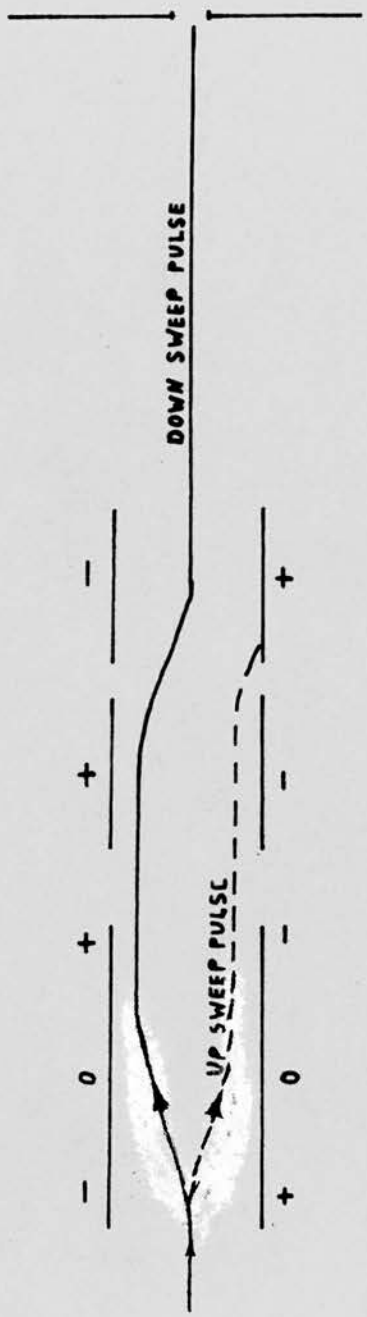

Fig. 16. ELIMINATING OF SUCCESSIVE BURSTS.

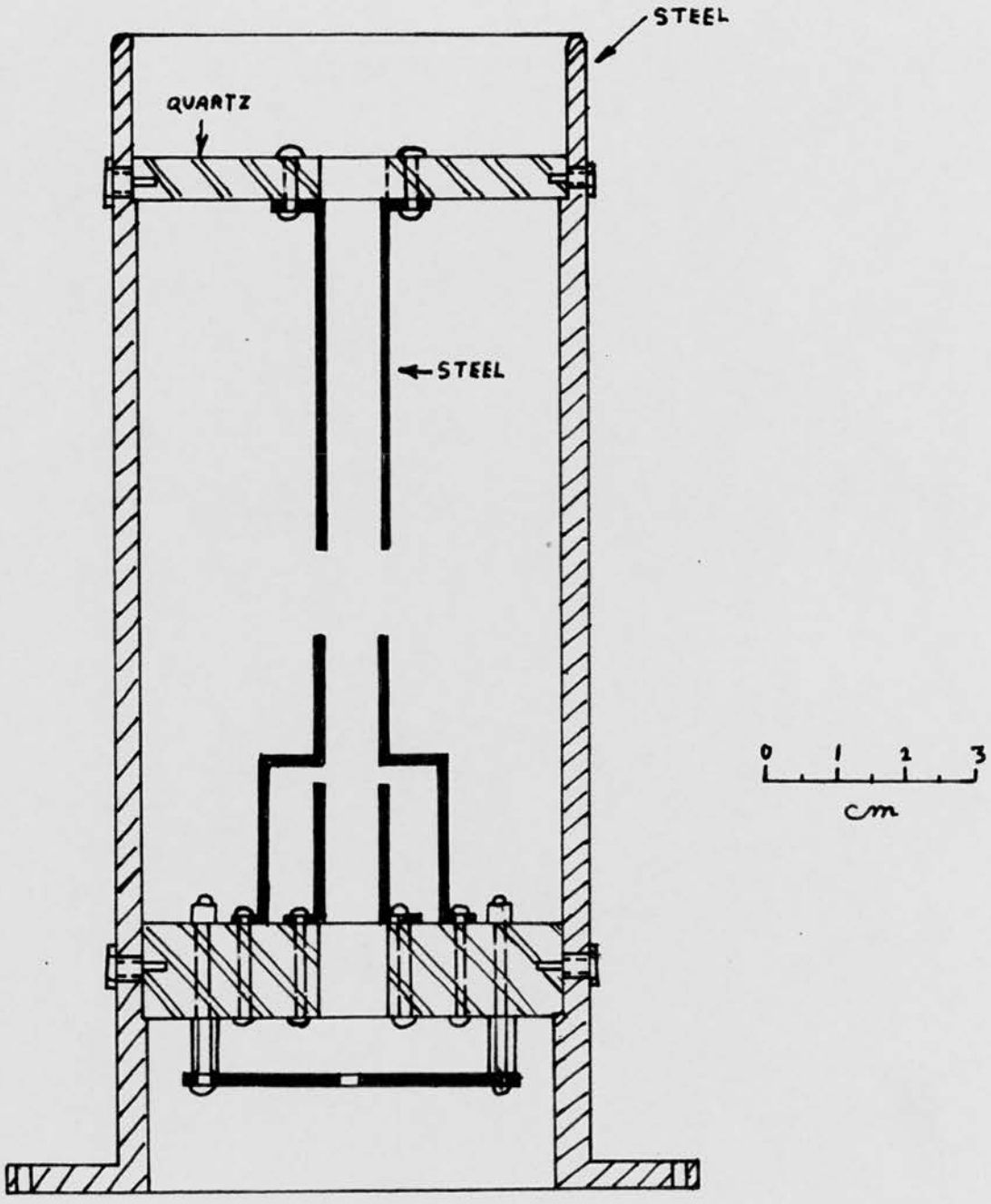

Fig. 17. THE PULSE SYSTEM.

the aluminium aperture, maintained at zero potential, and supported by the second quartz insulator. The diameter of the aperture is 4 mm., which was found to be the optimum size for passing the d.c. beam. The two quartz insulators and the deflection plate assembly are fixed in a steel cylinder which ensures good alignment.

Assume that a deuteron beam of 20 keV, with a diameter of 1 mm., enters the deflection system. The beam velocity is $v_o \approx 1.5 \cdot 10^8$ cm./sec. An r.f. field of 5 keV peak voltage with a frequency of 4MHz would, according to equation (24) produce a pulse duration of

$$\Delta t_o = \frac{2 \cdot 20 \cdot 10^3 \cdot 0.8}{2\pi \cdot 4 \cdot 10^6 \cdot 5 \cdot 10^3} \cdot \frac{0.4 + 0.1}{5(5 + 2.8)} \approx 3 \cdot 10^{-9} \text{ sec.}$$

The r.f. oscillator is a 4MHz oscillator with a peak voltage adjustable between zero and 15 kV. As the r.f. field is increased the burst duration is reduced until it reaches the limit due to the energy spread as explained above. Increasing the r.f. field beyond the limit will only reduce the peak ion current.

It can be shown that the bias voltage required on the refractor plates is

$$U = \frac{2 \Delta y_{screen} E.d}{e\ell^2} \qquad (30)$$

where U = voltage between plates,

ℓ = length of each of the refractor plates.

Thus, $U \approx 3$ kv.

The refractor power supply is adjustable from zero to +5kv. The plates indicated with negative polarity in Fig. 16 are at ground potential.

3.5. The Electronic Equipment

The block diagram of the experimental system is shown in Fig. 18.

The 40 MHz oscillator, the probe and the focussing power supplies are fed by a 220v supply through an isolating transformer. The transformer secondary has a centre tap connected to the pre-acceleration voltage. As mentioned before, this is a 1:1 transformer designed by Ferranti, with a maximum insulation of 30 kV, and an output power of no more than 1 kwatt at a temperature of 50°C.

The 40 MHz oscillator is the same type as used in the main H.T. set, designed by Philips (Fig. 19).

The probe and the focussing power supplies are both +5 kV supplies with an output current of about 10 mA. The two power supplies (Fig. 20) are of the bridge type. The transformer gives a

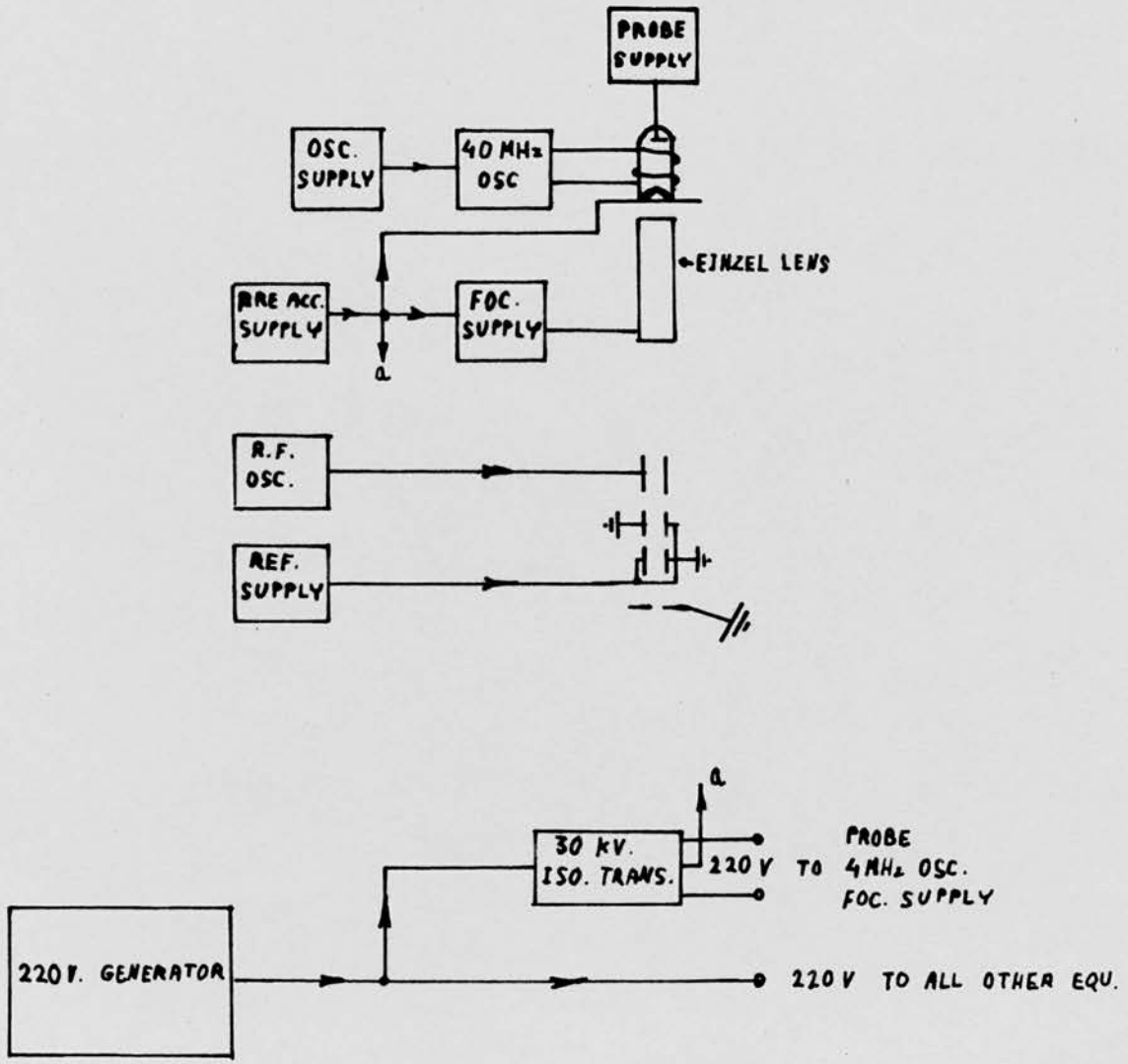

Fig. 18 BLOCK DIAGRAM OF EXPERIMENTAL SYSTEM

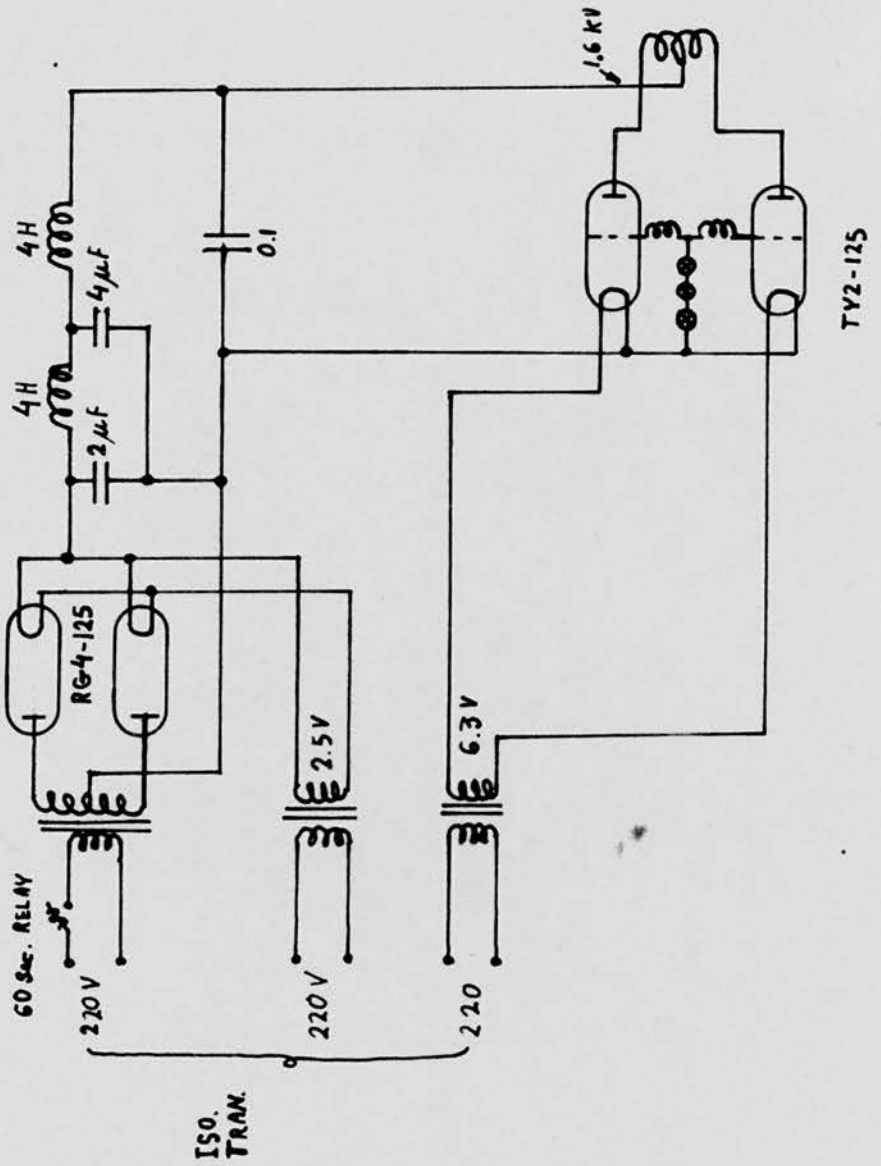

Fig. 19. 40 MHz. OSCILLATOR.

maximum 5000 volts output voltage and is fed from a variac which enables the output voltage to be adjusted from zero to 5 kV. It is preferable to use selenium rectifiers in the terminal rather than silicon ones, because of the danger of breakdowns due to high voltage surges in the terminal.

The pre-acceleration power supply is a +20kV supply with a 10 mA output current. The high voltage is achieved by a quadrupler circuit (Fig. 21). Assuming a load current of 5mA at 15 kV output voltage, the ripple is

$$U_r = \frac{I}{f.c} \qquad (31)$$

where I = load current,
f = main frequency,
c = capacitance.

$U_r \approx 200$ V, which is 1.3 % of the d.c. voltage. The output is adjusted by changing the primary voltage by means of a variac.

The R.F. oscillator for the deflector plates is shown in Fig. 22. It is a push-pull oscillator with two TY2-125 valves capable of giving an output power of about 300 watts and a peak voltage of 20 kV on the secondary of the step up r.f. transformer. The tank coil is supported by a quartz plate in order to reduce dielectric losses. The frequency of this oscillator is about $4MH_z$ and can be adjusted by altering the length of the coaxial

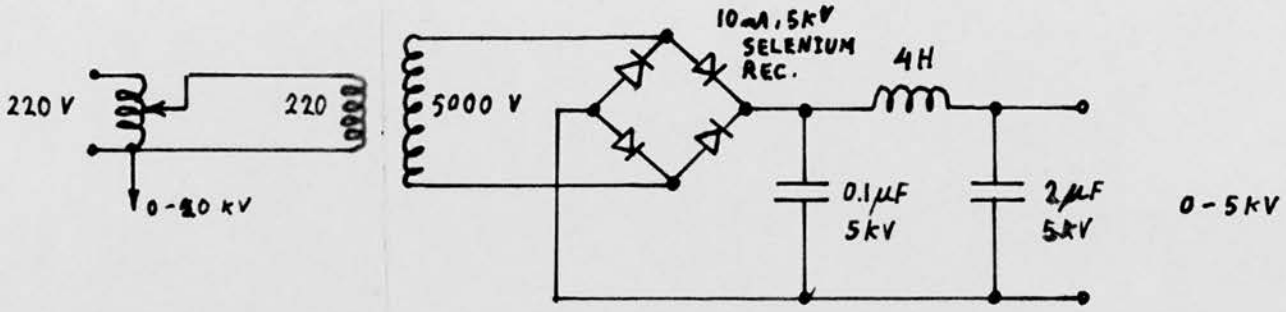

Fig. 20. PROBE & FOCUSSING POWER SUPLIES

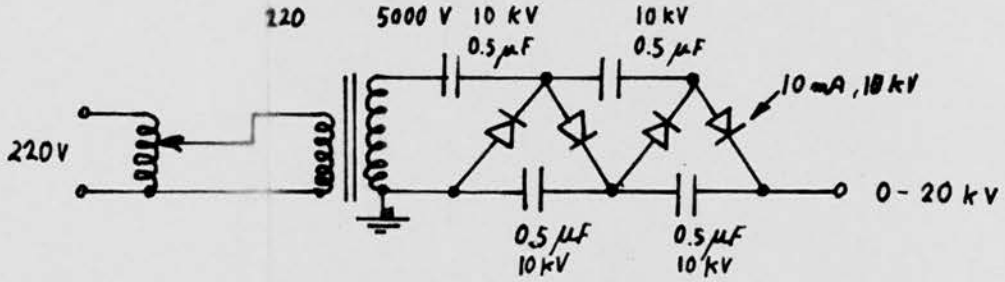

ALL RECTIFIERS ARE 10 mA 10 kV SELENIUM RECTIFIERS

Fig. 21. PRE ACCELERATION POWER SUPPLY

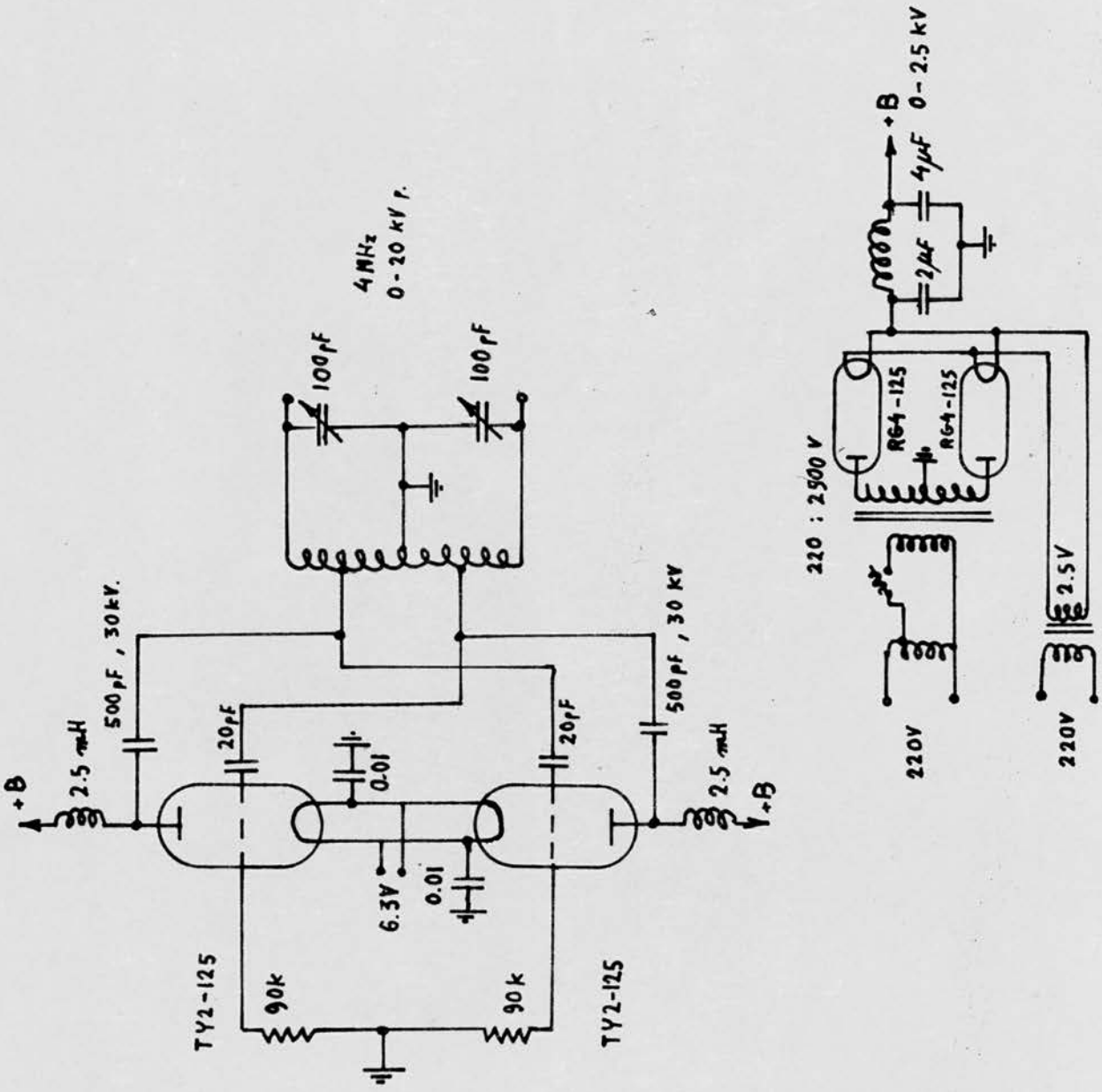

Fig. 22 DEFLECTION OSCILLATOR.

cables leading from the oscillator to the deflector plates since they act as parallel capacitors.

The refractor power supply (Fig. 23) is a simple half-wave rectifier 5 kV supply, capable of giving an output current of up to 10 mA.

The focussing Einzel lens and the pulsed section are located in one aluminium cylinder (Fig. 24) surrounded by an evacuated ceramic cylinder. All the voltage connections are on the top flange, as can be seen from Fig. 24. As most of the voltages are between 5 and 20 kV, and some are of high frequency, special insulators have been designed. These are all P.T.F.E. insulators (Fig. 25) with high dielectric constant, low high frequency losses, and low vapour pressure, important for the maintaining of high vacuum. The insulators showed excellent performance with voltages up to 30 kV. Fig. 26 is a photograph showing the top flange and insulators.

3.6. Results with the Experimental System

Results were obtained in two stages. The first was to check the quality of the beam at different distances from the Einzel lens. The diameter was measured by examining the discoloured area produced by the beam, on a steel target below the lens. First the pulsing section was omitted

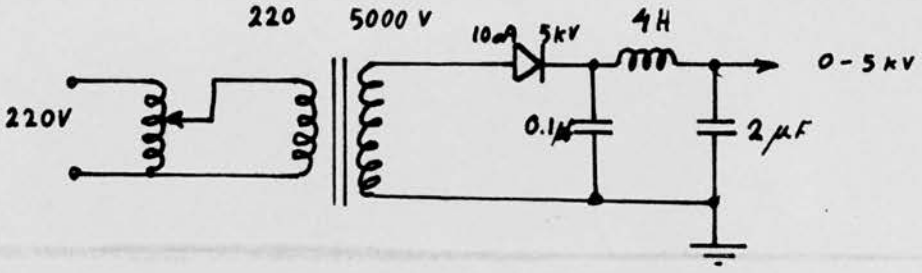

Fig. 23. REFLECTOR POWER SUPPLY

FIG. 24. The Aluminium Cylinder

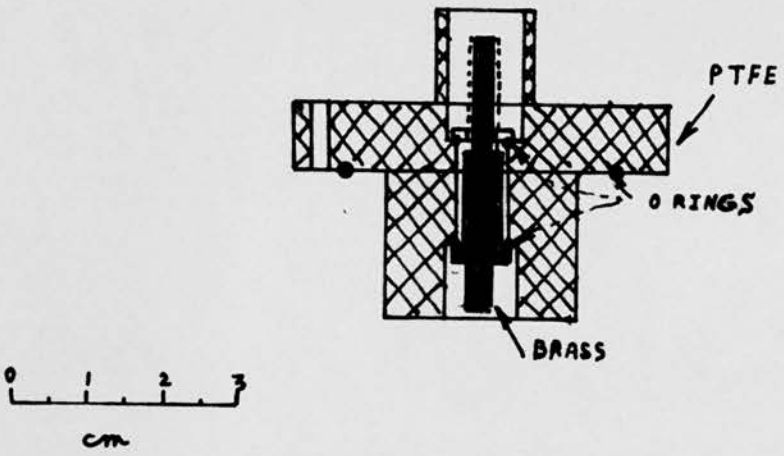

Fig. 25 THE PTFE INSULATOR.

FIG. 26 The Top Flange

and then inserted to check for any aberration of focussing due to this section. At best, the beam diameter was found to be less than 1 mm. The diameter changed little with distance from the lens or with the energy of the beam. The second stage consisted of putting the deflection section inside the system and obtaining a pulsed beam. The pre-acceleration energy was about 15 keV in order to work with the same condition as would hold in the main set. The pulse duration was measured by means of a Tektronix sampling oscillograph. The target was found to pick up signals from both the ion source and deflection oscillators so that it had to be surrounded by a special screen (Fig. 6) with only the one ground, connected from the oscillograph. In order to minimize the parasitic capacitance at the target, it was isolated from the bottom flange by a quartz tube, 5 cm. long. Assuming a target area of 5 cm^2 the parasitic capacitance is about 1 pF. The sampling oscillograph has an input impedance of 50 ohms giving a time constant of the order of 5.10^{-11} sec.

An r.f. field was applied to the deflector plates after adjusting the focussing voltage to obtain a maximum d.c. beam on the target. The burst duration could be adjusted from about 160 nsec. to a minimum of about 3 nsec. Any further

change of the r.f. field reduced the peak current in the pulse without changing its duration. Because of the low sensitivity of the sampling unit (0.2 $^{mA}/_{cm}$ with a load of 50 ohms), it was not possible to measure the dependence of burst duration on the peak current.

4. PULSING OF THE MAIN SET

4.1. General

The experimental system produced a d.c. or a pulsed beam with a well focussed image about where the aperture is located. This beam is to be fed into the accelerator. The experimental system, without any modification, was located at the top of the accelerator column, although the first accelerator electrode was replaced by a shorter one, of 55 cm. length. The d.c. or pulsed beam could only be focussed on the target, 4 meters below the ion source, by means of a second focussing after the aperture. This focussing is done in the gap between the aperture and the first acceleration electrode.

4.2. The Focussing of The Beam

The final arrangement at the terminal of the pulsed generator is shown in Fig. 27. The beam leaving the aperture enters the gap between the edge of the aluminium cylinder and the first accelerating electrode. The focussing effect between two coaxial cylinders has already been explained in part 3. The focussing is independent of the distance between the two cylinders, but depends on the internal diameters. If the two cylinders have the same diameter the beam particles

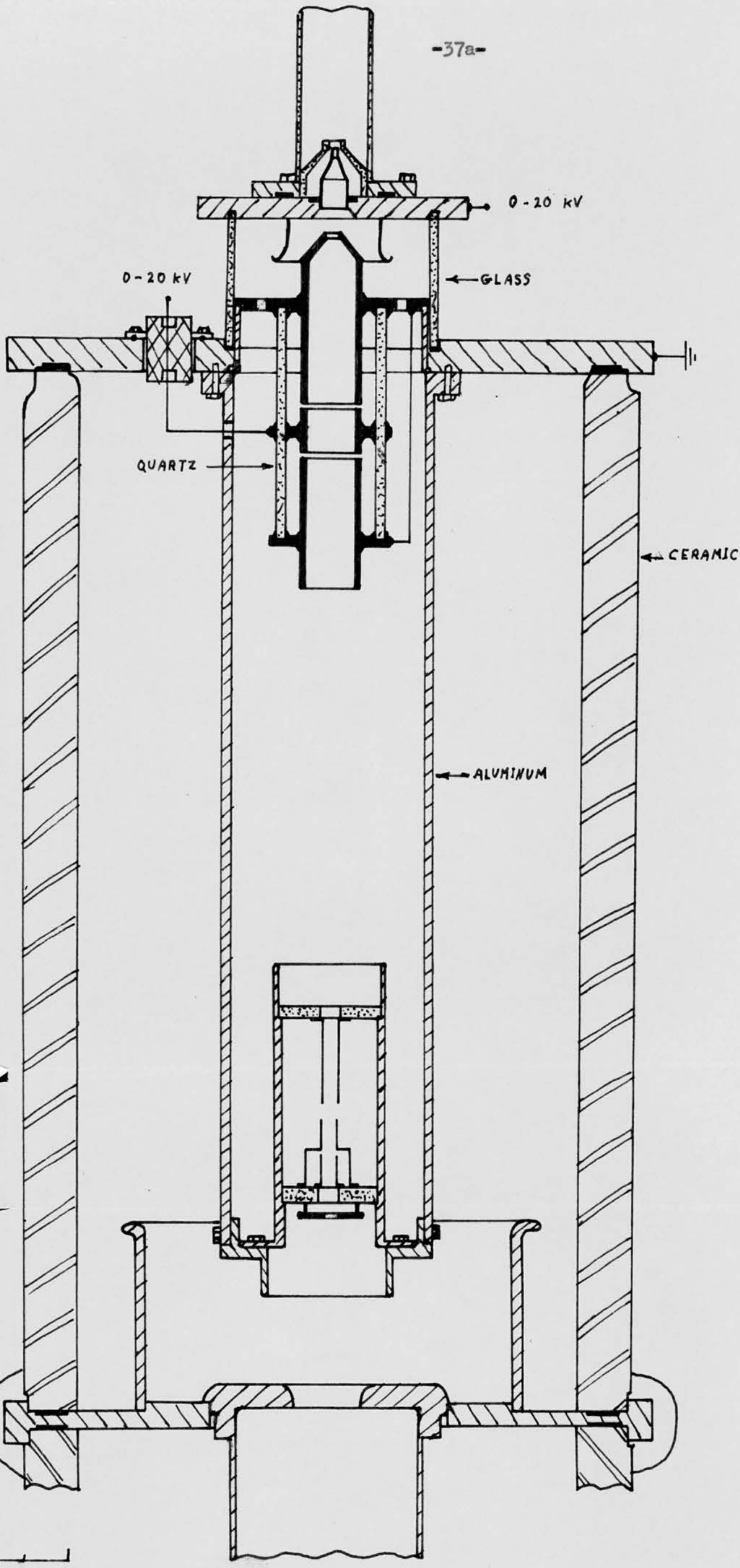

Fig. 27. THE PULSED TERMINAL.

are first focussed and then defocussed when approaching the second cylinder. As the particles gain energy while moving towards the second cylinder, the defocussing effect is only a secondary one. The effect could be minimized by reducing the diameter of the second cylinder. In the present case the use of a smaller diameter was found to be of great advantage. The diameter of the first cylinder is 7 cm., and the diameter of the first acceleration electrode about 4 cm. Assuming a total accelerating voltage of 500 keV and a pre-acceleration energy of about 20 keV, it can be seen from Fig. 10 that the image is about 40 cm. from the edge of the aluminium cylinder. The pre-acceleration voltage is adjusted to the value which will give a focussed beam within the gap between first and second acceleration electrodes. This gap produces a final focussing of the beam on the target. As the voltage ratio on these two electrodes is constant (2:1) (Fig. 3), the image formed on the target will not be affected by changing the overall accelerating voltage.

4.3. Results

The methods described in connection with the experimental system were used to examine the beam from the main set. The diameter of the beam on the target was found to be about 2 mm. Because of the high energy of the beam particles the diameter was measured by observing the glow produced by the beam on a quartz target. Deuterons were accelerated during these tests. The deuterium for the ion source was contained in a small metal cylinder and passed through a nickel leak for purification.

The accelerated beam is composed of several components in addition to the deuterons. These are mainly hydrogen and deuterium ions, as shown in Fig. 28. In order to obtain only one of these components on the target, the beam was deflected 30° by a magnetic field. The burst duration was measured by a sampling oscillograph connected to an isolated target, located beyond the analyzing magnet. With a new canal in the ion source and after careful adjustment of the different focussing voltages, the burst duration obtained was of about 3 nsec., with a peak current of a few hundred microamperes. The acceleration voltage was about 500 keV. For these measurements the refractor bias was maintained at 3 kV in order to obtain only one of the two successive pulses on the target.

The same electronic equipment was used as with

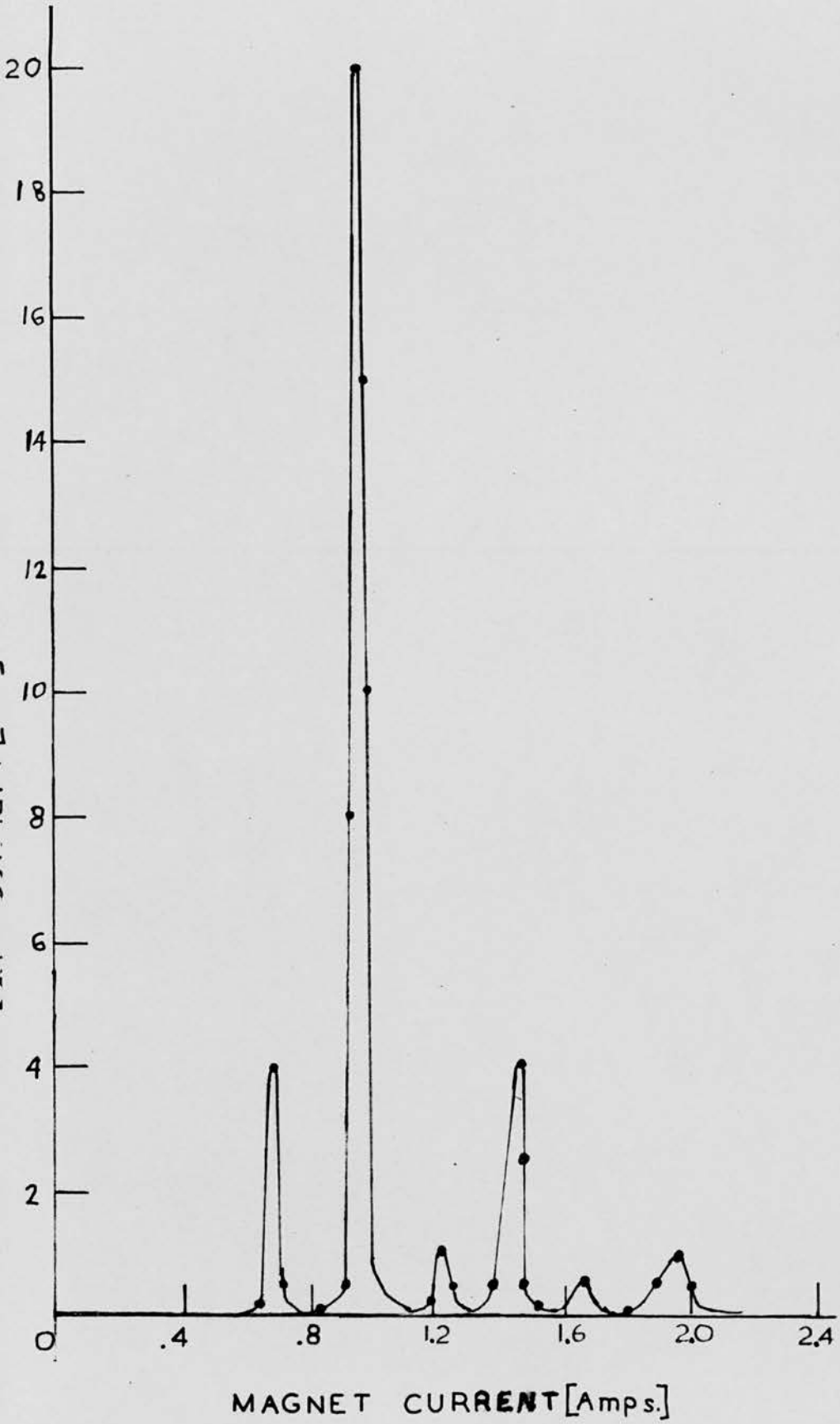

Fig. 28. ION CURRENT DISTRIBUTION.

the experimental system. Control of the units on the high voltage terminal was performed by means of string drives and slow speed motors remotely controlled.

5. ZERO TIMING SYSTEM

5.1. General

In a time-of-flight experiment it is necessary to obtain a time zero signal at the time of arrival of an ion burst at the target. Several methods for producing the timing pulse are described below.

It has been shown that each time the r.f. field across the deflector plates reaches its zero potential, a burst of ions passes through the aperture. After a certain time, depending on the acceleration voltage, this burst will reach the target. It is possible to pick up the oscillator signals, amplify them, and produce a zero-time signal corresponding to the time at which the r.f. field passes through zero. The time taken by the ions to travel through the accelerator is about 1 microsecond. The energy stability of the accelerator is no better than 1% , so that the uncertainty in time will be of the order of 5 nsec. In order to obtain a resolving time of a few nanoseconds the jitter in the zero timing pulse should not exceed 1 nsec., so that a system of this type is not practicable.

Another method for obtaining a zero timing pulse consists of connecting the target to ground

through a small impedance, z, so that whenever a burst of ions reaches the target, a voltage pulse U_z will appear across the impedance z.

$$U_z = I_p \cdot z \qquad (32)$$

I_p = burst peak current.

As the zero timing signal is on the target itself, it is difficult to measure the mean current during the experiment. This system could not be used when a time pulse is desired before the beam reaches the target, as is necessary when a bunching magnet is introduced.

A more practicable method is based on passing the particle beam through a hollow metal cylinder, located at the point where the time measurement is required. The beam induces a charge on the cylinder resulting in a fast voltage pulse being produced. This, after amplification, could be used as a zero time pulse. The main disadvantage of this system lies in the dependence of the output pulse on the burst peak current, so that a time jitter could be produced whenever the accelerated beam current is changed. This last system was used in our case.

5.2. Description of The System

If the length of the cylinder is equal to, or larger than the length of the burst of beam, a quantity of charge equal to the burst charge will be induced on the cylinder.

The burst charge is given by

$$Q = I_p \, \Delta t_o \qquad (33)$$

where Δt_o = duration of burst.

The length of the burst is given by

$$L = 0.042 \, \Delta t_o \sqrt{\frac{E}{M}} \quad [cm] \qquad (34)$$

where E = acceleration voltage in keV.
M = particle mass in a.m.u.
Δt_o = pulse duration in nsec.

Assuming a deuteron beam accelerated to an energy of 700 keV and a burst duration of 3 nsec. the corresponding length will be

$$L = 0.042.3 \sqrt{700/2} \approx 2.5 \text{ cm.}$$

A brass cylinder 5 cm. long was chosen in order to obtain maximum pulse amplitude under most operating conditions. The pulse amplitude will be:

$$V_z == \frac{Q}{C} \qquad (35)$$

where c is the parasitic capacitance of the cylinder plus the input capacitance to the amplifier following the pick-up. This neglects the real part, R_i, of the input impedance to the amplifier, since,

$$R_i C \gg \Delta t_o \qquad (36)$$

In order to minimize c, the cylinder was isolated from both the analyzing magnet and the target by quartz tubes. The mechanical arrangement is shown in Fig. 29. Assuming a peak current of 30 μA with a duration of 3 nsec., the charge induced on the cylinder is of the order of 10^{-13} coulomb.

The rise time of the pulse is equal to the burst duration which is 3 nsec. Assuming a capacitance c, of 10 pF, the pulse amplitude will be U = 10 mV.

The pre-amplifier connected to the system should have the following properties.

(a) A rise time of a few nsec.

(b) A noise level low enough to eliminate any uncertainties in time measurement.

(c) A low input capacitance, so as to obtain maximum amplitude from the induced charge.

(d) A low output impedance to feed a wide band amplifier.

A cascade transistorized pre-amplifier was found to be best suited to the above requirements. The pre-amplifier[15] (Fig. 30) consists of two low noise, high frequency, Texas Instruments GM0290 transistors in a cascade connection, and one fast transistor (Texas Instruments 2N1141) as an emitter follower. The input capacitance to the amplifier is[16]

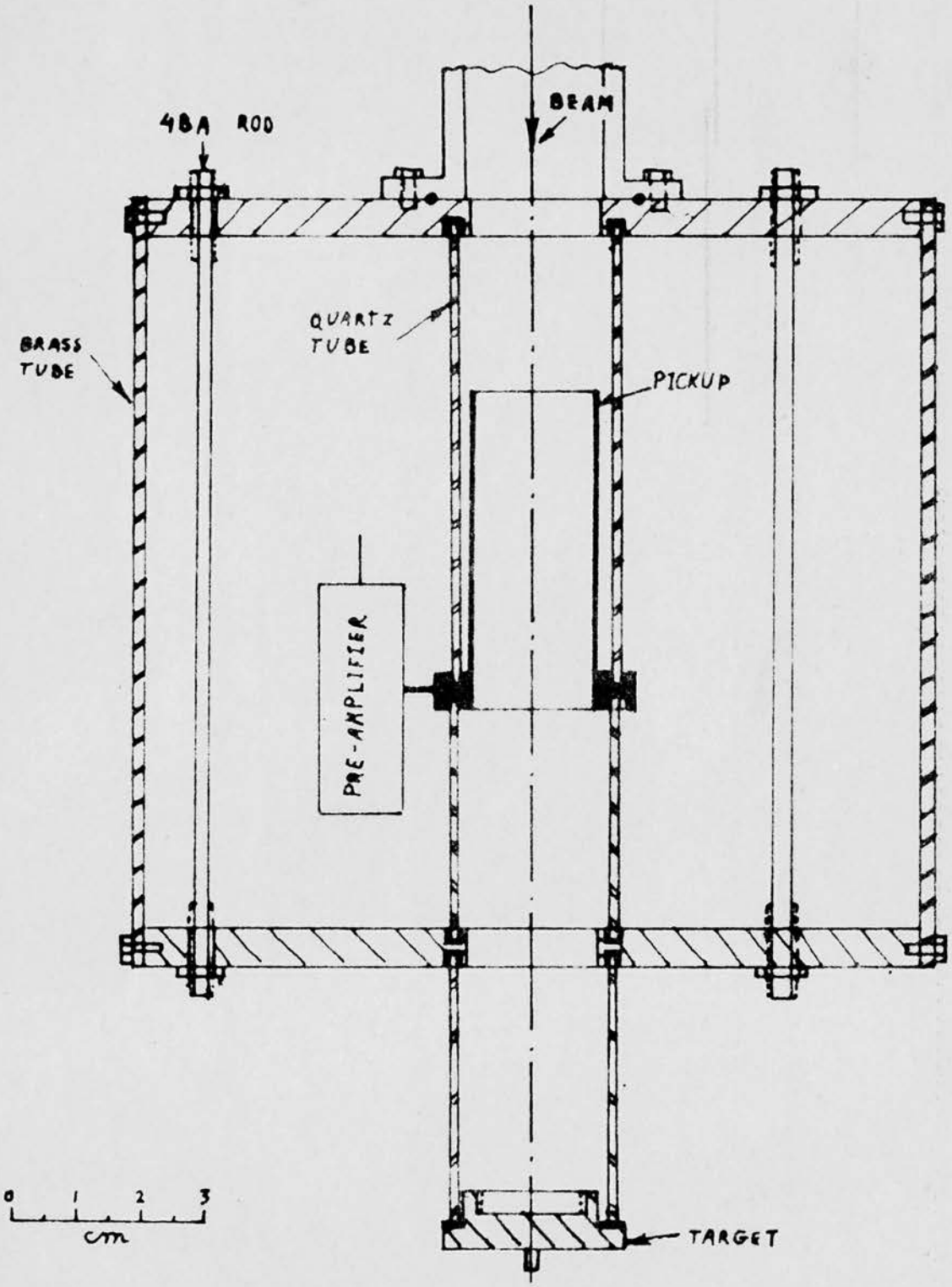

FIG. 29. The Pickup System.

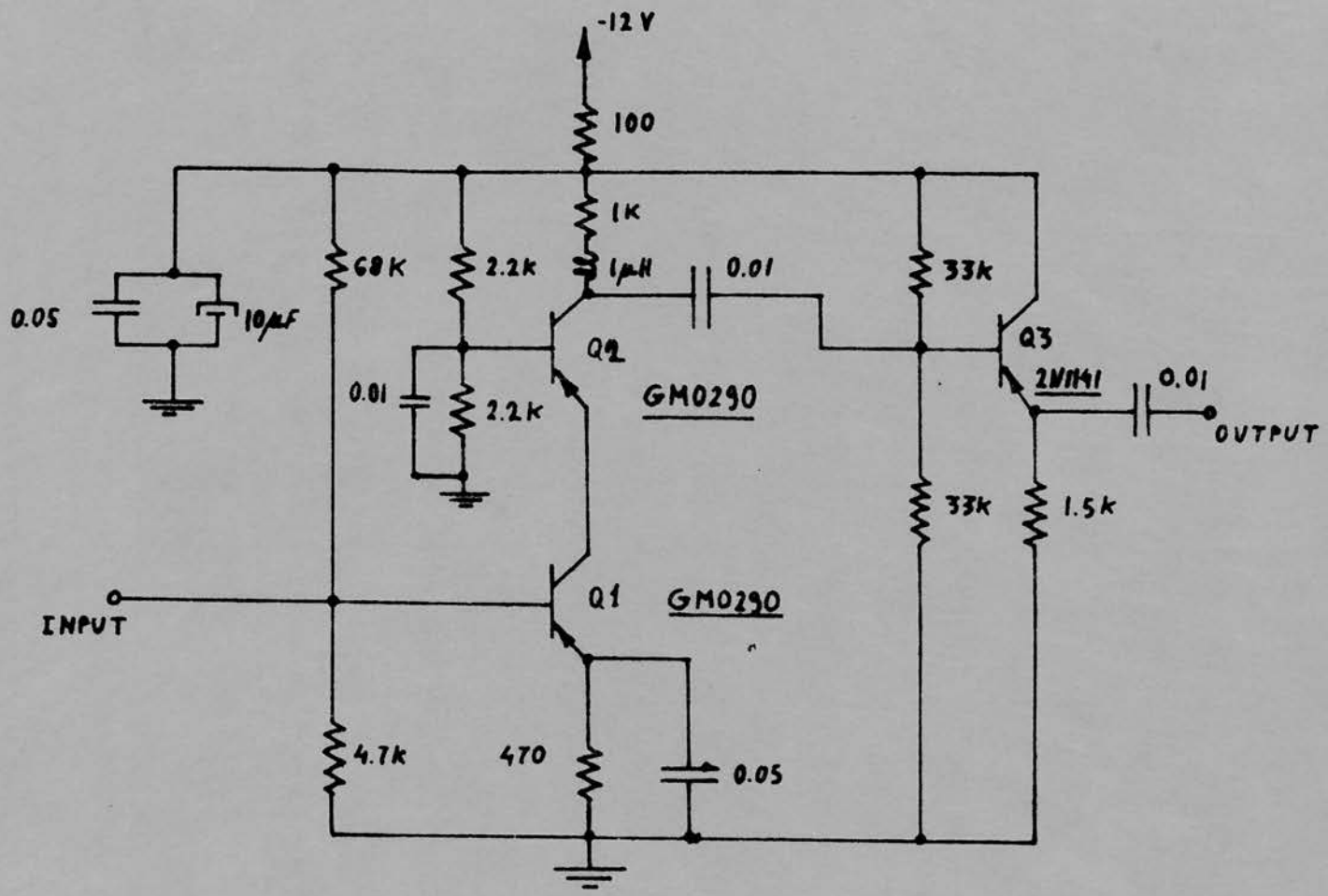

Fig. 30. Pickup pre-amplifier

$$C_i = C_{b'\ell} + C_{o_b}(1 + g_m R_L) \qquad (37)$$

where $C_{b'\ell}$ = emitter-base diffusion capacity of Q_1.

C_{o_b} = deflection-layer capacity of the collector base junction of Q_1.

$g_m = \frac{\alpha_o}{r_e} \approx \frac{1}{r_e}$ of Q_1,

when α_o is the low frequency, common base current gain, r_e is the intrinsic emitter resistance, r_e = 26 ohm per 1 mA emitter current. R_L = load impedance of Q_1.

In a cascade connection, R_L is equal to the input impedance, R_i, of Q_2. For a common base connection this impedance is

$$R_{i_2} = r_e + r_{bb'}(1 - \alpha) \qquad (38)$$

where $r_{bb'}$ is base-spreading resistance of Q_2. In our case $r_{bb'}$ is about 50 ohm and $\alpha = 0.99$, therefore $r_e \gg r_{bb'}(1 - \alpha)$. Because of a very low input impedance to Q_2, $R_{12} \approx r_e$, the input capacitance to Q_1 is equal to:

$$C_i \approx C_{b'e} + 2C_{o_b} \approx 5 \text{ pF} \qquad (39)$$

Assuming a parasitic capacitance to the pick-up cylinder, including a stray wiring capacitance of about 5 pF, the total capacity, C, on the cylinder is $C \approx 10$ pF. To minimize the stray wiring

capacity, the base of the first transistor is soldered to the cylinder. The input resistance to Q_1 is :

$$R_{in} \approx r_{bb'} + \beta r_e \qquad (40)$$

where β is the current gain of the common emitter stage with a shorted load circuit

$$\beta = \frac{\alpha}{1 - \alpha} \qquad (41)$$

In the case described $\beta \approx 100$, $r_e \approx 13\,\Omega$, thus

$$R_{in} \approx 1350\,\Omega \ .$$

The input time constant, $R_{in}.C$, is of the order of 13 nsec. and therefore the amplitude of the input pulse will be determined by the input capacitance (according to (35)).

The voltage gain of the first two transistors is

$$A = \frac{\beta R_{L_2}}{r_{bb'} + r_{b'\ell}} \qquad (42)$$

where R_{L_2} = the load of Q_2

$r_{b'\ell} = r_e(\beta + 1)$.

For a 1 kΩ load resistor, $A \approx 60$.

The frequency range , f, of the pre-amplifier is

$$f \approx \frac{1}{2\pi R_{L_2} C_o} \qquad (43)$$

where C_o is the output capacitance of Q_2

plus input capacitance of Q_3, equal to about 3pF. Thus $f \approx 50\ MH_z$, or a rise time of about 6 nsec. An inductance was put in series with R_{L2} in order to improve the frequency response. The last stage is an emitter follower with a high input impedance,

$$R_{in} = r_{bb'} + \beta(r_e + Re) \qquad (44)$$

(where R_e = the emitter resistor),

a low output impedance,

$$Ro = \frac{R_g + r_{bb'}}{\beta} + r_e$$

(where R_g = output impedance of Q_2)

and a voltage amplification of almost 1.

The frequency response of the emitter follower is good enough not to affect the total frequency response. The overall amplifier has a voltage amplification of 50 with a rise time of about 5 nsec. The input noise is between 15 to 30 microvolts.

The output of the pre-amplifier is fed into two wideband amplifiers connected in series, with a total amplification of 100 and a rise time of 3nsec.

Assuming a mean pulse with a duration of 3nsec. and a peak current I_p, the zero timing pulse after the wideband amplifier will have the amplitude of

$$U_o = 50.100. \frac{I_p \Delta t_o}{C} \qquad (45)$$

The overloading amplitude from the amplifier is 10V so that the amplifier will be generally overloaded, giving a 10V output with a rise time of 3 nsec.

In order to obtain a resolving time, T_r, the rise time of the pulse triggering the time-to-amplitude converter, following the system, should not change by more than T_r, over the range of beam current to be employed. The minimum triggering level needed for the time to amplitude converter (T.T.A.C.) being used in conjunction with the system, is about 1V. Thus the minimum beam current for which the time error is less than T_r, will be

$$I_p \geqslant \frac{1}{A} \frac{Am.C}{\Delta t_o} \cdot \frac{t_r}{T_r} \qquad (46)$$

where Am = pulse amplitude required to trigger the T.T.A.C.
t_r = Rise time of the pre-amplifier and amplifier.
A = amplification of pre-amplifier and amplifier.
C = input capacitance to pre-amplifier.
Δt_o = burst duration.
T_r = allowed error in resolving time.

When allowing a time error of 10^{-10} sec. the minimum current in our case is about 30 microampere.

The output noise is about 100 mV which is 10 times smaller than the required triggering pulse.

6. APPLICATION

6.1. The Electronic Units, Circuits, Assembly.

After the quality of the pulsed beam had been determined by electronic means it was necessary to study the properties of the Pulsed Accelerator in a number of physical experiments. To that aim a time-of-flight spectrometer was developed. The block diagram of the electronic set-up is given in Fig. 31.

The essential problem in fast neutron time-of-flight experiments, is to measure the time taken by a neutron to travel a fixed distance from the accelerator target to the neutron detector. In our case, using the pulsed beam, this is the time interval between the instant a burst of beam strikes the target and the instant a resulting neutron reaches the detector. The detector is a fast neutron liquid scintillator (NE 213), attached to a fast photomultiplier (56AVP). As the liquid scintillator is also sensitive to γ-rays, the input to the time-to-amplitude converter will contain an unwanted background of γ-ray pulses. Two inputs are fed into the time-to-amplitude converter, one from the photomultiplier, the other from the zero timing channel which was discussed in detail in part 5. If the γ-ray background is

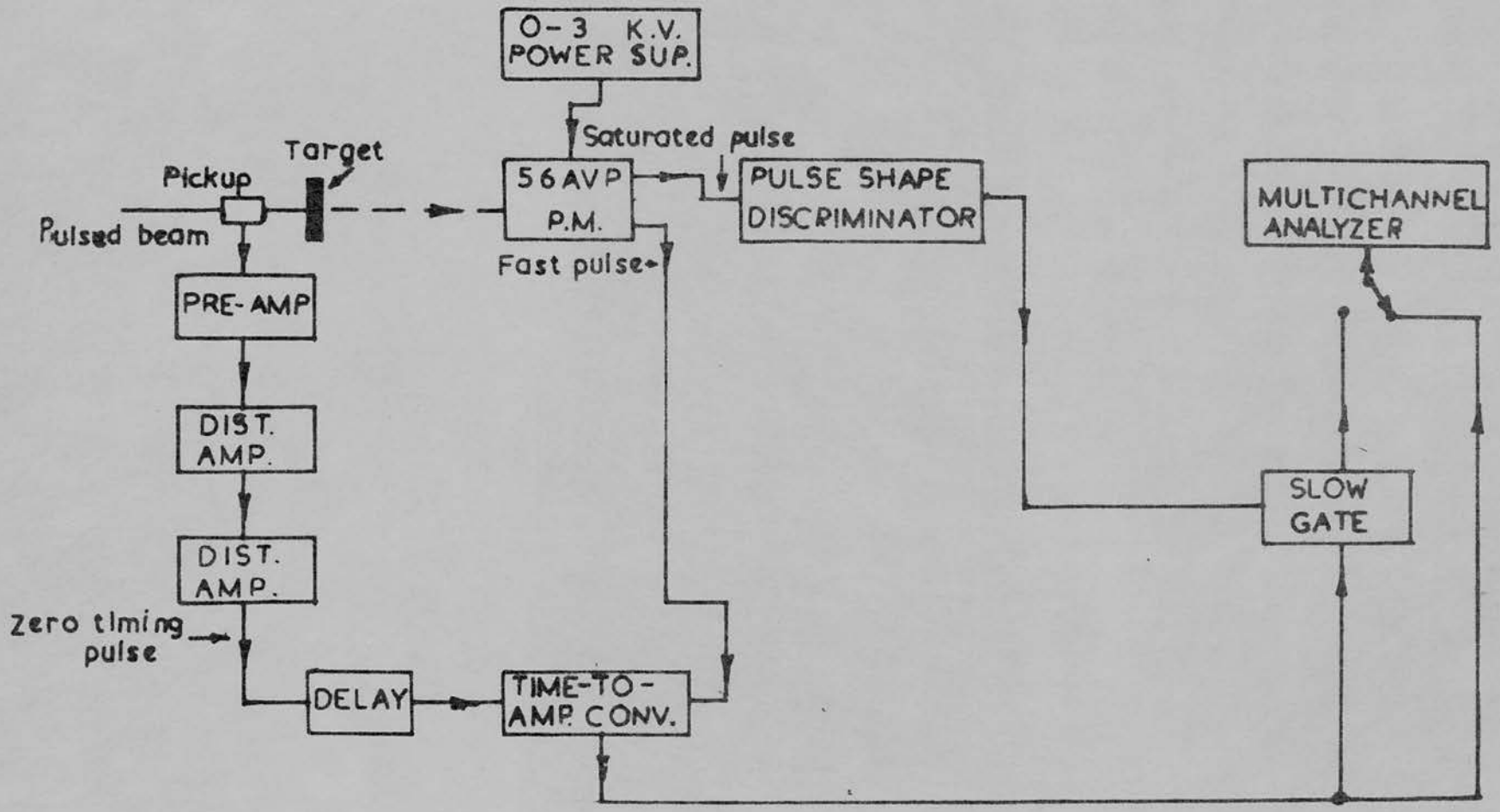

Fig.31. Block diagram of the electronic setup

too high, a pulse shape discriminator system may be added. The output from the time-to-amplitude converter is fed into a standard slow gate, controlled by the pulses from the pulse shape discriminator system, so that the spectrum displayed on the multichannel pulse height analyzer is due only to the detection of neutrons. When the γ-ray background is sufficiently low the pulse discriminator may be omitted.

6.2. The Time-To-Amplitude Converter[15]

In any ordinary time-to-amplitude converter the amplitude of the output pulse is proportional to the time interval between the two input pulses independent of their order of arrival. Thus many of the output pulses will actually be due to negative time measurements. If only one of the two inputs would trigger the converter while the second would reset it, only time intervals with the required sign will be measured. As each of the neutron pulses is associated with a zero timing pulse, the photomultiplier pulse is used to trigger the time-to-amplitude converter, and the zero timing pulse, after being delayed, is used to reset it. In this way only positive time intervals are measured and many unwanted output pulses, due to zero timing pulses which have no associated neutron

pulses, are ignored.

The time-to-amplitude converter (Fig. 32) is based on a 6BN6 sharp cut-off pentode[17]. The input to the GBN6 is a square pulse, fed onto the first grid, with very fast rise and fall times and a constant amplitude of +3V. The width of the pulse is equal to the time interval between the arrival of the two inputs to the converter. Therefore, a constant current will flow through the anode, charging the anode capacitance, during this interval, giving an output voltage pulse proportional in amplitude to the measured time.

The square pulse is formed by means of a very fast bistable tunnel diode multivibrator. The tunnel diode, Q_4, is a 5mA diode with the characteristics shown in Fig. 33. The tunnel diode in parallel with a 330 ohm resistor is connected as the collector load of an NPN 2S131 fast transistor, Q_3. The collector d.c. current is about 3mA, adjustable by means of a variable 1KΩresistor in its base. As the voltage drop across the tunnel diode in its first stable state (A in Fig. 33) is about 25mV, most of the collector current will flow through the tunnel diode according to the load line AC. If a minimum current of -2mA is injected into the tunnel diode cathode the operating point will switch from A to C, according to line "a" in Fig. 33. The voltage on the collector will then change from 25mV at A to 425 mV at C. A

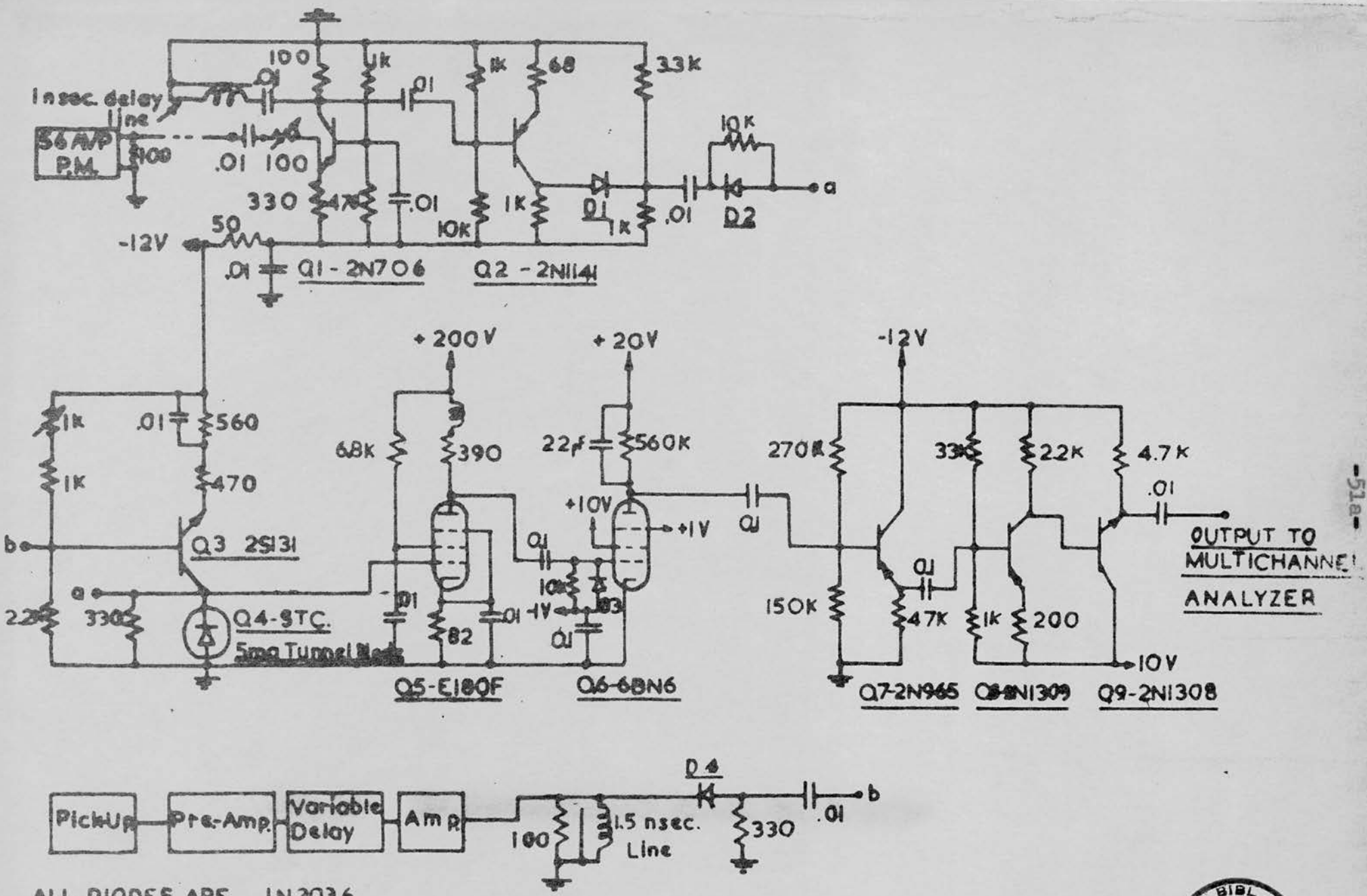

Fig.32. Time-to-amplitude converter

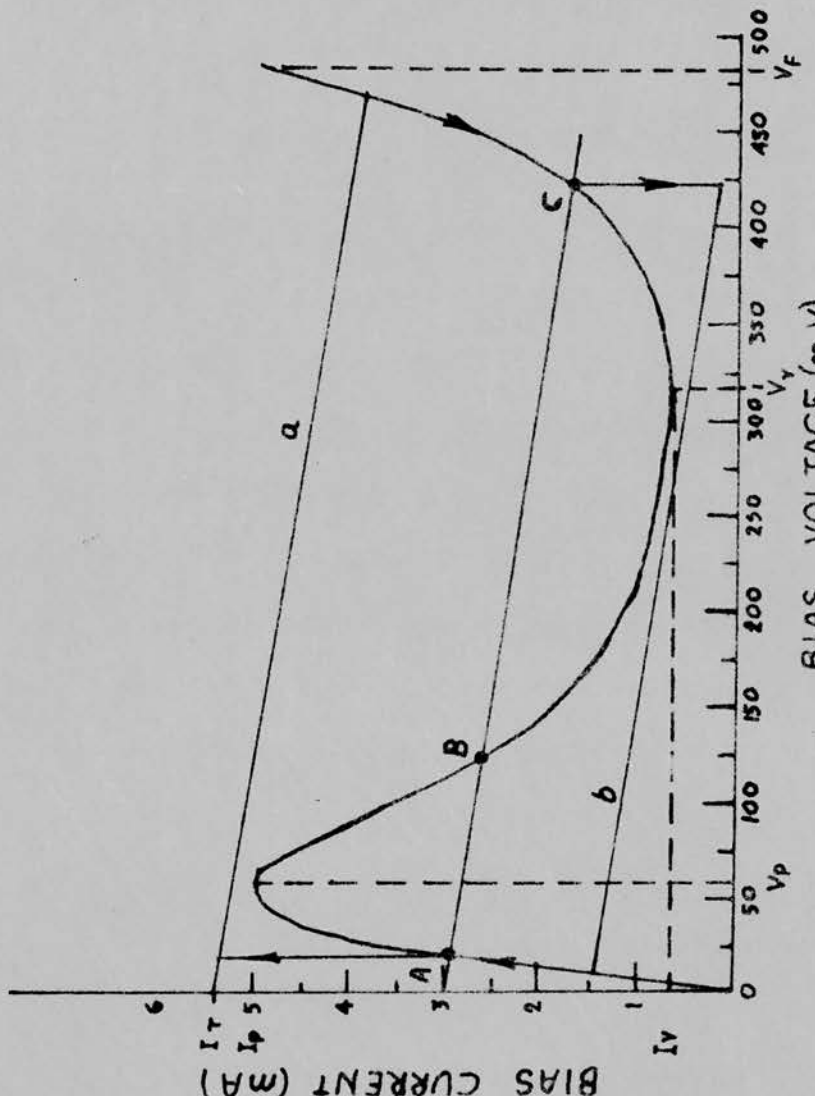

FIG. 33. The Characteristics of the Tunnel Diode.

minimum positive current of 15 mA is needed to switch the tunnel diode back to its original position (along line "b"). This can be achieved by a negative voltage pulse applied to the base of Q_3. The corresponding collector current will be

$$i_c \approx {}^{e_i}/_{R_e} \qquad (47)$$

where i_c = the collector current.

e_i = the amplitude of the input voltage signal.

R_e = the a.c. emitter resistor, 470 Ω in our case.

It can be seen from line "b" that most of the change in the collector current will affect the tunnel diode. Thus the change in collector current required to trigger the tunnel diode back to its original position is less than 2 mA. As the d.c. collector current is about 3 mA, the transistor will not reach its cut-off position and no extra delay will be introduced. The transistor Q_3 is in the common emitter configuration with current feedback in the emitter and a low load on the collector, so the voltage amplification is less than 1. Under these conditions the transistor is a current amplifier and has a very good frequency response when driven by a voltage source[16]:

$$f_i \approx \frac{1}{2\pi C_{b'e} r_{b'e} \dfrac{R_g + r_{bb'} + R_e}{R_g + r_{bb'} + r_{b'e} + \beta R_e}} \qquad (43)$$

$$f_o = \frac{1}{2\pi R_L C_o} \qquad (49)$$

where

f_1 = input circuit upper limit frequency response.

f_o = output circuit upper limit frequency response.

$C_{b'e}$ = emitter base capacity.

$r_{b'e} \approx \frac{0.027 \cdot \beta}{I_e}$ ohm.

I_e is the emitter d.c. current in mA.

β is the low frequency common base current gain.

R_g = generator impedance

$r_{bb'}$ = base spreading resistor

R_e = emitter resistor

R_L = collector load resistor.

C_o = collector capacitance + parasitic capacitance at the collector junction.

As one of the two inputs to the converter is connected to the collector and the other to the base of the same transistor, they are well isolated. The tunnel diode is switched from one operating point to the other, and back to the first, only by two negative inputs, of which the first is a current pulse fed to the cathode of the tunnel diode, and the second, a resetting pulse, is a voltage pulse applied to the base of the transistor. The output is a negative pulse, taken from the common junction of the collector and tunnel diode, with an amplitude of about 0.4 V and a duration equal to

the time interval between the two inputs. The rise and fall times of this pulse are about 2 nsec, depending on the shape of the input impulses.

As the input required for the 6BN6 tube is a positive pulse with an amplitude of 3V, the output from the tunnel diode is amplified by a E180F tube (Q_5).

The rise time at the anode of the E180F is

$$t_r = 2.2\ RC \qquad (50)$$

where R = anode load resistance (390 Ω in our case).

C = anode capacitance, about 10 pF.

With an r.f. choke at the anode of the E180F tube, the square pulse driving the 6BN6 will have rise and fall times of about 4 nsec. The output pulse from the time-to-amplitude converter is a negative pulse with a slow fall time of about 10 μsec, determined by the anode load of the 6BN6, the input impedance of the amplifier following it, and the anode capacitance. The amplitude corresponding to a time of 100 nsec. is about 0.4V. The multichannel pulse height analyzer (Laben-Mod. A51 Cise.) requires a positive input pulse which is obtained from a three stage linear amplifier (Q_7, Q_8 and Q_9) with an amplification of about 10.

The photomultiplier pulses require to be shaped to make them suitable for triggering the converter at the junction of the tunnel diode and

and the transistor Q_3. As has already been shown, this point should be driven by a current pulse with a minimum peak of 2 mA and a minimum duration which can be calculated from the characteristics of the tunnel diode:

$$t \approx \frac{C(U_B - U_A)}{I_r - I_p} , \qquad (51)$$

C being the total capacitance across the tunnel diode.

The output from the photomultiplier is taken from the 13th dynode, with a rise time of about 2 nsec. and an amplitude of a few volts across a 100 Ω load. For best resolution it is advisable to use a pulse shaper of the zero time crossing type[18, 19]. As the burst duration obtainable from the accelerator in the case described is no better than a few nsec, it was decided to use a pulse shaper of a simpler type. The pulse shaper consists of two transistors, Q1 and Q2 (Fig. 32). The first is a fast NPN transistor type 2N706 connected in the common base configuration. The input impedance to this stage,

$$R_{in} = r_e + r_{bb'} (1 - \alpha) \qquad (52)$$

is of the order of a few ohms. Therefore a variable 100 ohm resistor is connected in series with the emitter to match the 100 ohm coaxial

cable leading from the photomultiplier to the shaper input. The output of this stage is a 100 ohm shorted line giving output pulses whose duration is 2nsec. The emitter d.c. current is about 10 mA. As the input to this stage is a positive pulse, the transistors will reach the cut-off position when the input is larger than 0.5V, giving a positive output pulse with an amplitude of about 0.5V. This pulse is applied to the base of a PNP fast transistor, type 2N1141. The emitter current of this transistor is about 10 mA,of which, 3mA passes through the fast diode D1 (Fig. 32). When a positive pulse of more than 450 mV is applied to the base of Q2 the diode D1 will enter the cut-off region and a negative current of 3mA will flow through the diode D2, triggering the tunnel diode. D2 prevents the resetting of the tunnel diode by positive pulses at the output of the shaper, and so prevents the production of spurious pulses in the converter. The resetting pulse, coming from the zero timing system, after a delay of 100 nsec., is shaped by a shorted line, to a duration of 3 nsec., and is fed to the base of the transistor Q1 (Fig. 32) through a fast diode D4. This diode eliminates from the zero timing system positive pulses that would trigger the time-to-amplitude converter, allowing only negative resetting pulses to pass.

The power supply for the time-to-amplitude converter and the zero timing pre-amplifier is shown in Fig. 34.

The performance of the time-to-amplitude converter was tested by means of the electronic set-up shown in Fig. 35. The linearity was found to be better than 1% up to times of about 120 nsec. (Fig. 36). For a larger linear range the anode capacitance of the 6BN6 tube (Fig. 32), should be increased, too large an increase will reduce the amplitude of the output pulse from the 6BN6 tube to such a low value that extra amplification will be needed. The width at half-maximum of the spectrum of pulses from the time-to-amplitude converter was less than 1 nsec. A similar test was performed by means of a mercury relay pulse generator, and the resolving time was found to be better than 0.2 nsec. By disconnecting one of the inputs, it was shown that there is no appreciable intercoupling between the two inputs. This is due to the fact that there is only one input to the 6BN6 tube, connected to its first grid.

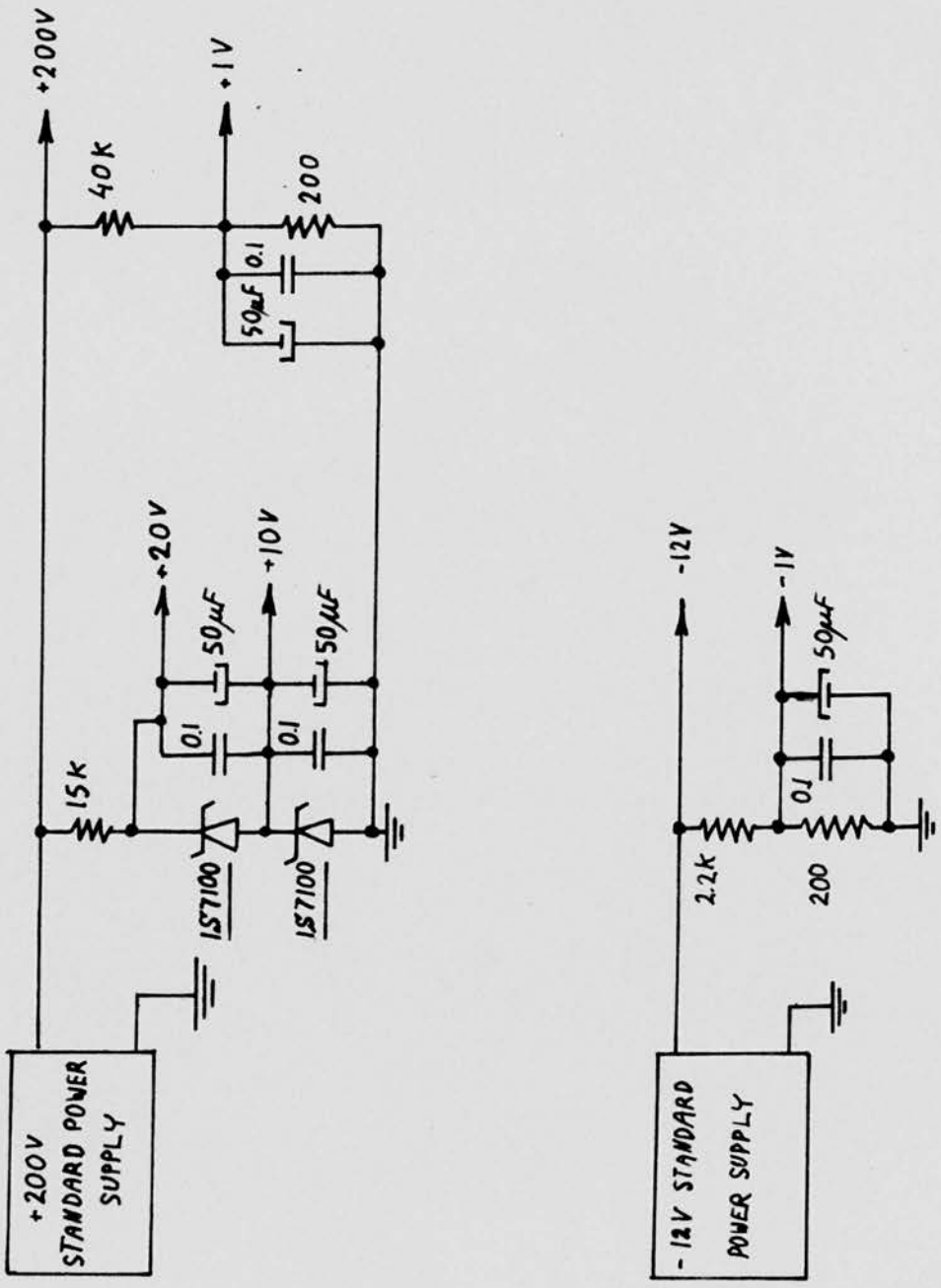

Fig. 34. THE T.T.A.C. POWER SUPPLY.

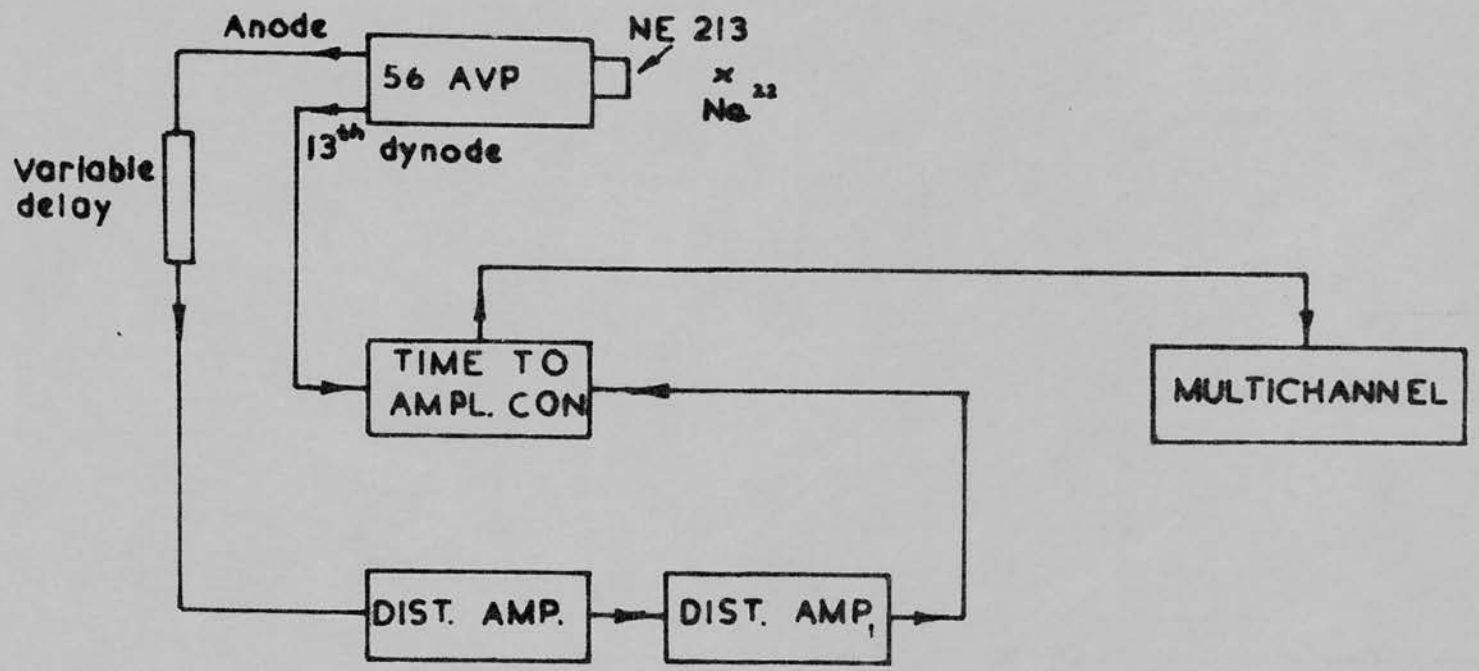

Fig. 35. Calibration setup

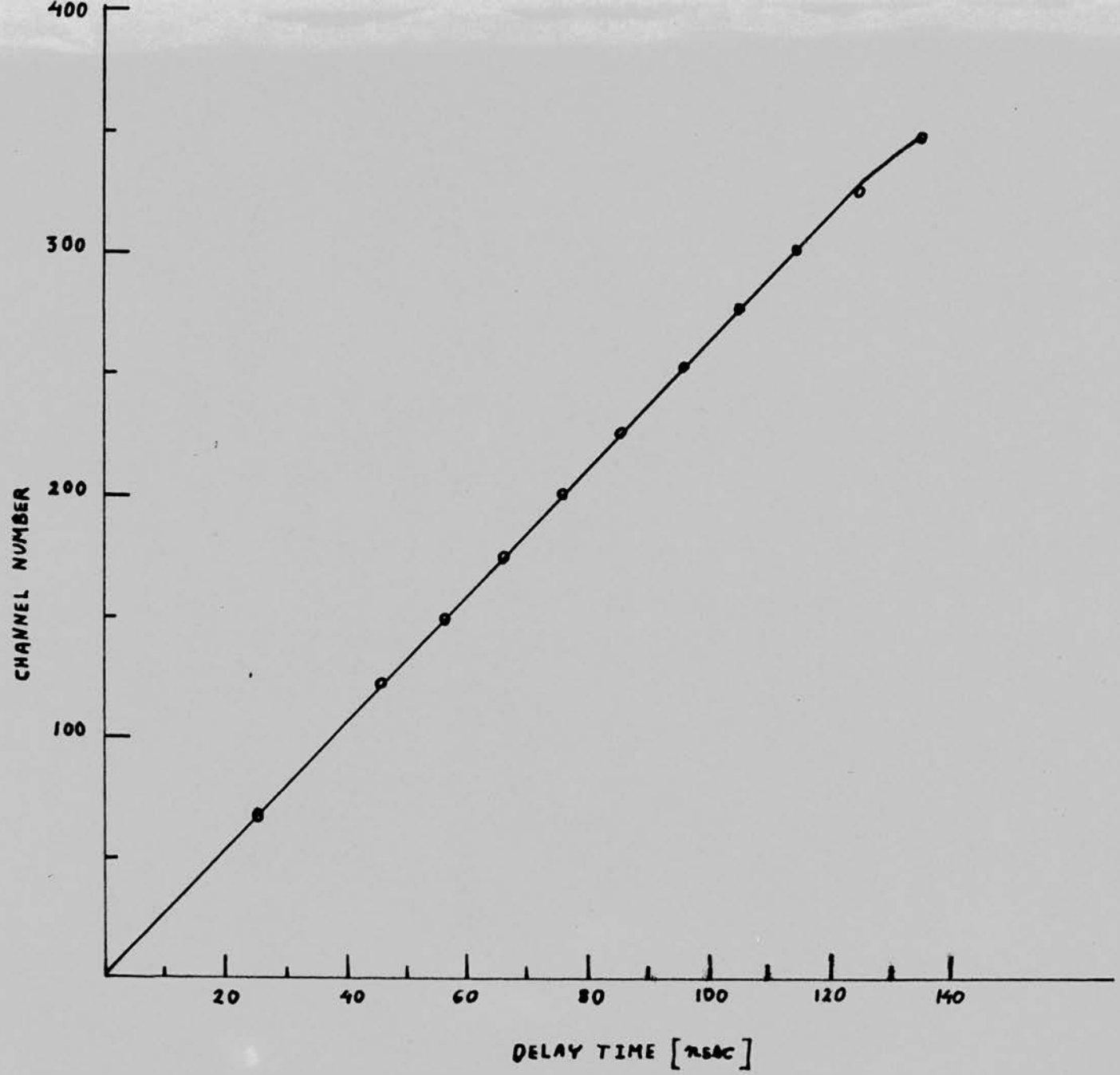

Fig. 36. CALIBRATION CURVE

6.3. The Pulse Shape Discriminator

A type 56AVP photomultiplier was used in the spectrometer. The photomultiplier circuit used to provide the pulse shape discrimination is shown in Fig. 37. The pulse shape discrimination[20, 21] is based on a saturation effect between the anode and last dynode of the photomultiplier, resulting in a pulse whose shape depends on whether neutrons or γ-rays were detected. (Fig. 38). After amplification by a linear amplifier with a long differentiation time constant (1500 μsec. in our case) and an integration time constant of 0.2 μsec, most of the γ-ray pulses are eliminated by pulse height discrimination. The remaining pulses, due to the detection of neutrons, control a slow coincidence gate which receives its input pulses from the time-to-amplitude converter (Fig. 31). The spectrum obtained on the multichannel analyzer, following the gate, is thus due solely to neutron pulses.

The diode OA10 in the photomultiplier circuit, cuts the negative part of the pulses at the last dynode, eliminating the possibility of overloading the linear amplifier following the photomultiplier. The output from the 14th dynode is a fast pulse with a rise time of about 2 nsec. and is used for triggering the time-to-amplitude converter.

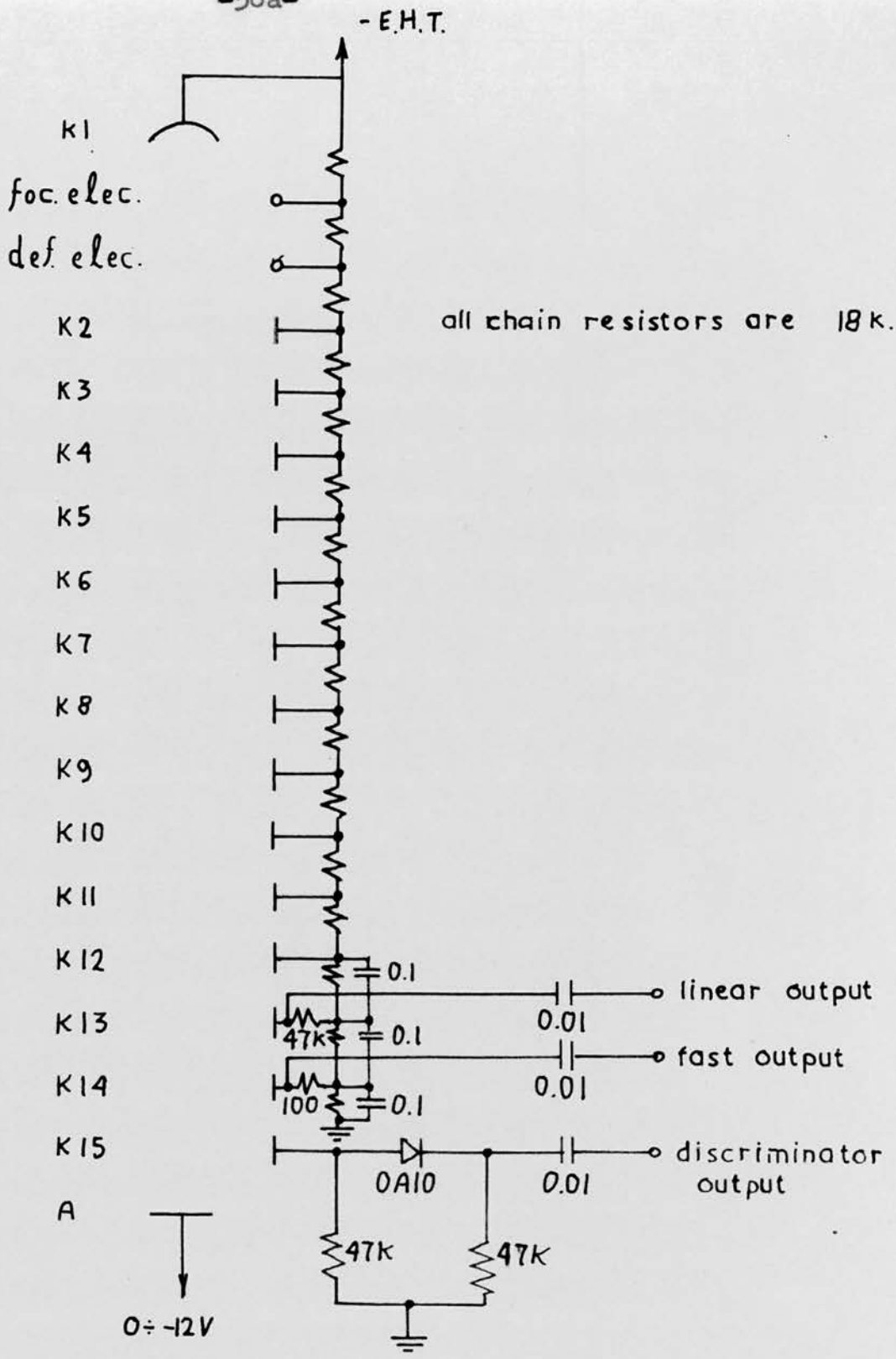

Fig. 37. PHOTOMULTIPLIER CIRCUIT.

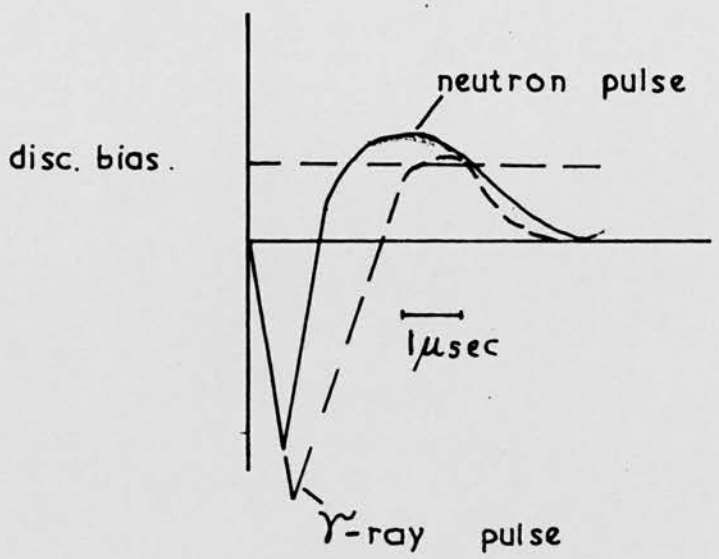

Fig. 38. DYNODE PULSE SHAPE.

6.4. Measuring of Burst Duration By Means of a γ-ray Spectrum.

The burst duration of a pulsed beam is best measured by measuring the width at half-maximum of a γ-ray time-of-flight spectrum from a target bombarded by the pulsed beam. If the resolving time of the spectrometer is shorter than the burst duration, this duration is equal to the half maximum width of the γ-ray spectrum.

The target in our case was a thick aluminium disc. A 500 keV proton beam with a peak current of a few hundred microamps. was used to bombard it. The results obtained are shown in Fig. 39. In order to draw an accurate time scale, two identical spectra, separated by 6.5 nsec., by passing the zero timing pulses along a delay line, were displayed on the multichannel analyzer (Fig. 39). The burst duration was found to be of the order of 3 nsec.

6.5. The Neutron Time-of-Flight Spectrum of The $D(d,n)He^3$ Reaction.

The $D(d,n)He^3$ reaction was the first to be examined, because of its high yield and the existence of only one neutron group. The target in this case was NaOD, prepared by mixing Na with

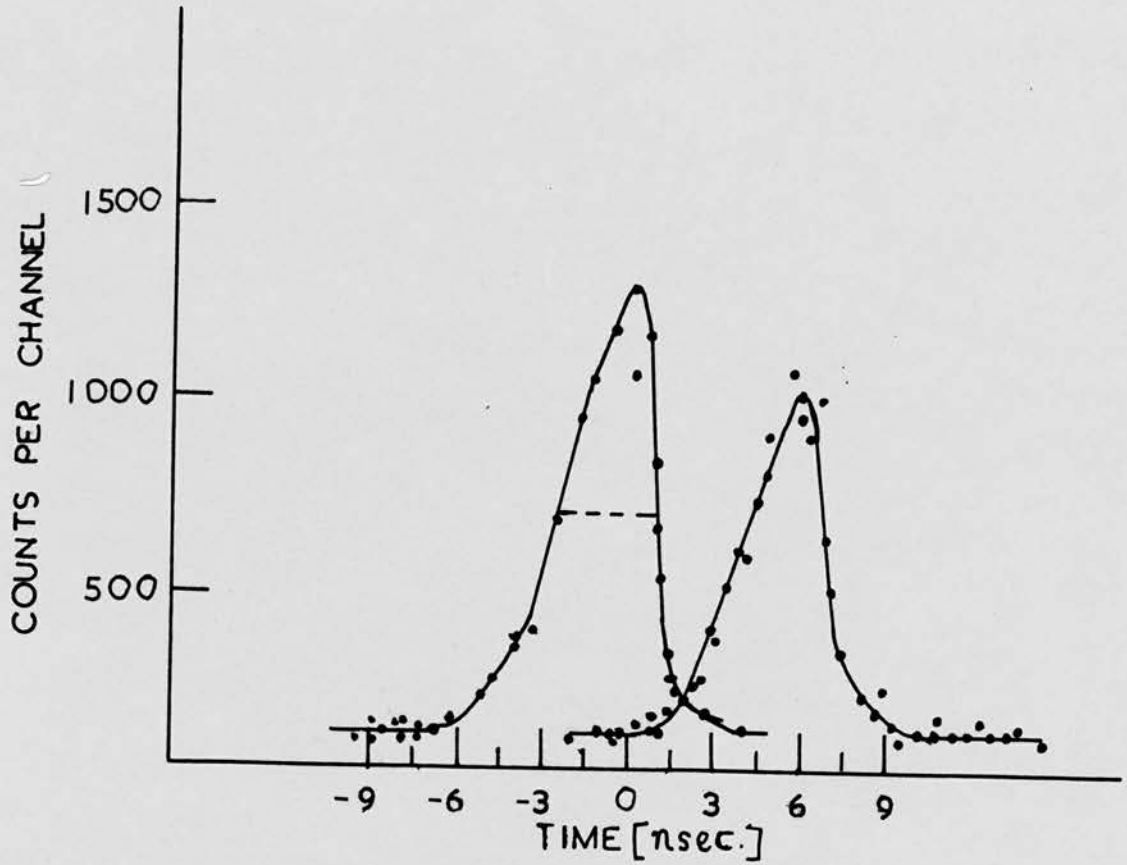

Fig. 39. γ RAY SPECTRUMS OF PROTONS BOMBARDING Al. TARGET.

heavy water on a brass plate and evaporating the residual water. A 600 keV deuteron beam with a peak current of a few hundred microamps was employed. The detector was maintained at an angle of 90° to the beam and at a distance of 25 cm. from the target. The neutron energy in this case[22] is 2.55 Mev. It could easily be shown that the corresponding time-of-flight is 12.5 nsec. The results obtained from this experiment are shown in Fig. 40. The smaller peak, in the spectrum, is due to γ-rays from carbon and other impurities on the target. The larger peak is the neutron peak separated from the γ-peak by 12.5 nsec. The burst duration of the deuterium beam, determined from this spectrum is of the order of 3 nsec.

Assuming a maximum deuteron energy spread of 600 keV, because of the thick target, the neutron energy spread[22] will be of the order of 0.15 Mev or a time spread at the detector of:

$$\Delta t = \tfrac{1}{2} \frac{\Delta E}{E} \cdot T \approx \tfrac{1}{2} \text{ nsec.} \qquad (53)$$

where Δt = the time spread.
T = neutron time of flight from target to detector.
E = neutron energy
ΔE = neutron energy spread.

This is much less than the burst duration and therefore the use of a target of finite thickness will not introduce an appreciable error in the estimate of burst duration.

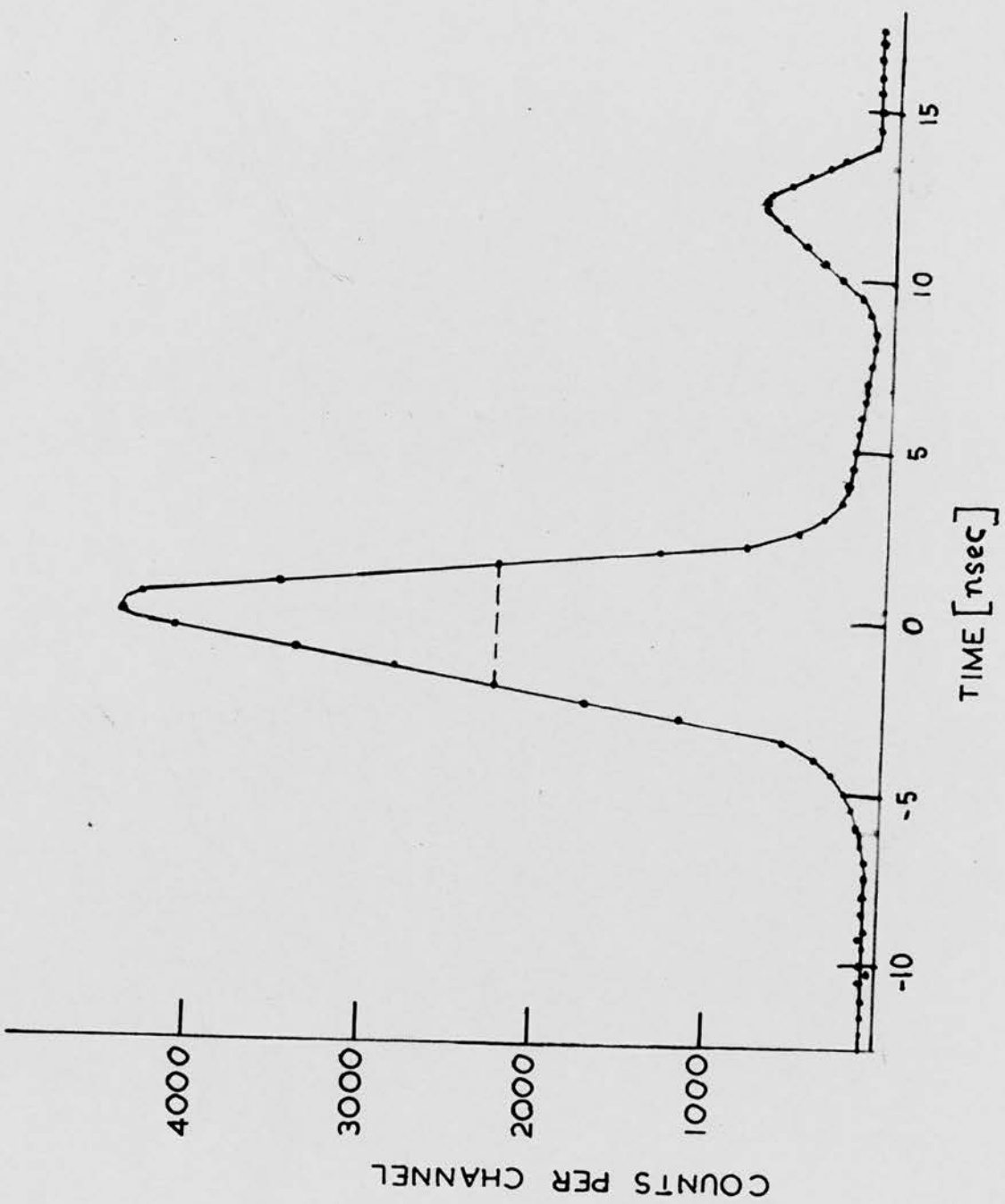

Fig. 40. NEUTRON SPECTRUM OF $D(d,n)H^3$ REACTION

6.6. The Neutron Time-of-Flight Spectrum from $B^{10}(d, n)C^{11}$.

The $B^{10}(d, n)C^{11}$ reaction has already been investigated by many workers and therefore it was decided to examine this reaction as a test of the pulsed accelerator.

C^{11} has excited states[23] at 2.00, 4.32 and 4.81 Mev. These, and the ground state, should be reached by the $B^{10}(d, n)C^{11}$ reaction when the deuteron energy is 600 keV. A B^{10} target was used which was bombarded for 3 hours, by a 600 keV deuteron pulsed beam with a peak current of a few hundred microamps. The detector was at a distance of 2 meters from the target and at an angle of 0^{o} to the beam. D. Vass[24] calculated the neutron energies and flight times for the different excited states at different angles and deuteron energies. The neutron energies for ground, first, second and third excited states are: 6.86, 4.95, 2.72 and 2.24 Mev. respectively. The corresponding flight times for a distance of 2 meters are: 55.20, 64.96, 87.62 and 96.48 nsec.

Results obtained from this experiment are shown in Fig. 41. Because of a high γ-background the pulse shape discriminator was used. To reduce the background of scattered neutrons coming from the walls, a paraffin wax shield was put around the

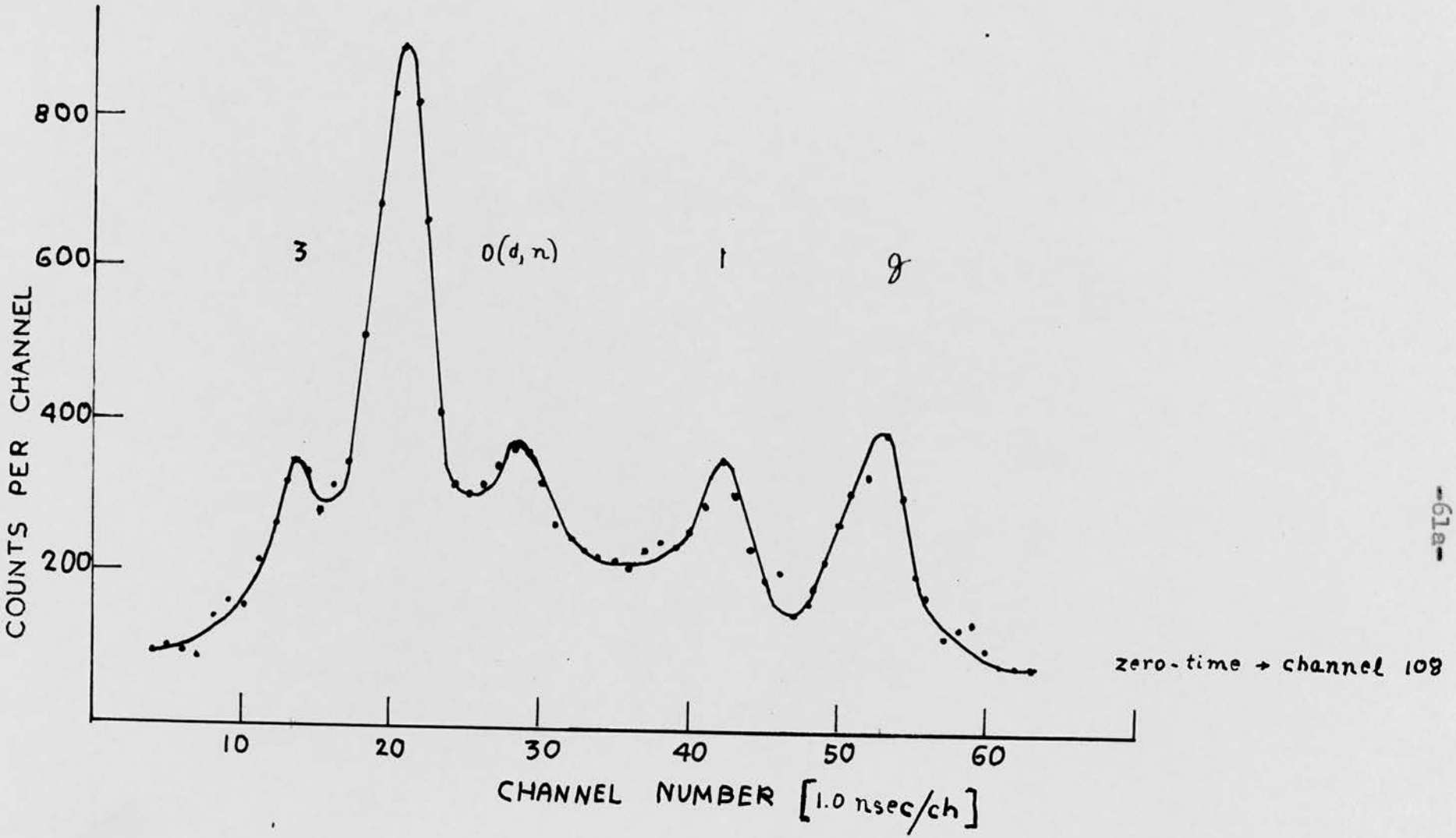

Fig. 41. NEUTRON SPECTRUM OF $B^{10}(d,n)C^{11}$ REACTION

detector. The spectrum obtained consists of 5 peaks. The first two correspond to the ground state and the first excited level. Some of the deuterons bombarding the target will be absorbed and the $D(d, n)He^3$ reaction will produce an additional peak. The time-of-flight for these neutrons, under the conditions described, is 78.9 nsec. Thus the third peak in the spectrum is due to the $D(d, n)He^3$ reaction. The other two peaks shown in Fig. 41 are from the formation of the second and third excited levels of C". These results agree with results obtained, under similar conditions, by C,H. Paris and P.M. Endt[25], who detected the neutrons by the recoil protons observed in nuclear emulsions.

6.7. The Neutron Time-of-Flight Spectrum from $B_e^9(d, n)B^{10}$ Reaction

Many experiments have been performed in order to study the energy levels of Boron 10. In spite of this there are some uncertainties about the existence of some levels. The well known levels accessible to the $B_e^9(d, n)B^{10}$ reaction with 600 keV deuterons, are at 0.72, 1.74, 2.15 and 3.58 Mev.[23] In addition, an energy level at about 2.86 Mev was reported by various people. All the evidence in favour of this level comes from the

$B^9(d, n)B^{10}$ reaction. Dyer and Bird[26] reported on the existence of a level at 2.85 Mev, after studying with nuclear emulsions the neutron emitted in this reaction. By the same method Genin[27] reported on the existence of a level at 2.95 Mev. The deuteron energies were of 600 keV in the Dyer's experiment and of 700 keV and 600keV in Genin's experiments. Reid[28] reported on a level at 2.88 Mev after using a recoil proton telescope to obtain the neutron spectrum produced by a 750 keV deuteron beam. Shpetnyi[29] studied the reaction with nuclear emulsion and found no evidence for the existence of an energy level around the 2.85 Mev. He performed his experiments with deuteron energies of 0.5, 1.0 and 1.6 Mev. Galloway and Sillitto[30] by studying the γ cascades found it possible that a 2.86 Mev level exists. G. Bradford[31] studied the γ-rays from $B^9_e(d,n)B^{10}$ and came to the same conclusion with a difference in the probability of exciting the proposed level. Coombe and Walker used a cloud chamber to examine the neutrons from the $B^9_e(d,n)B^{10}$ reaction at a deuteron energy of 80 keV. They found evidence to support the existence of a level at 2.9 Mev. They indicated that this level may be composed of two levels with energies of 2.7 and 3.1 Mev. The

most direct evidence for this level would be to obtain a neutron spectrum from the $B^{9}_{e}(d,n)B^{10}$ reaction. Evidence for this level from neutron spectra was inaccurate because of poor statistics. It was decided to study the reaction by a time-of-flight technique in two different ways. The first is by a time-of-flight experiment based on a d.c. deuteron beam and the second, by performing the time-of-flight experiment with a pulsed beam. D. Vass[24] after studying the neutron time-of-flight spectrum from the $B^{9}_{e}(d,n)B^{10}$ reaction, using a d.c. beam, found no evidence for the existence of any neutron group other than those corresponding to the four known levels of B^{10} at 0.72, 1.74, 2.15 and 3.58 Mev. Results obtained by means of the pulsed accelerator are shown in Figs. 42 and 43. The target was a thick beryllium metal disc, bombarded by a pulsed deuteron beam with an energy of 600 keV and a peak current of a few hundred microamperes. The detector was at a distance of 2 meters from the target and an angle of 0^{o}. The neutron energies corresponding to the ground state and the other four excited levels are[24]: 4.83, 4.15, 3.17, 2.77 and 1.37 Mev, and the corresponding times-of-flight for a distance of 2 meters are; 65.74, 70.94, 81.18, 86.80 and 123.30 nsec. In order to reduce the background to a minimum, the

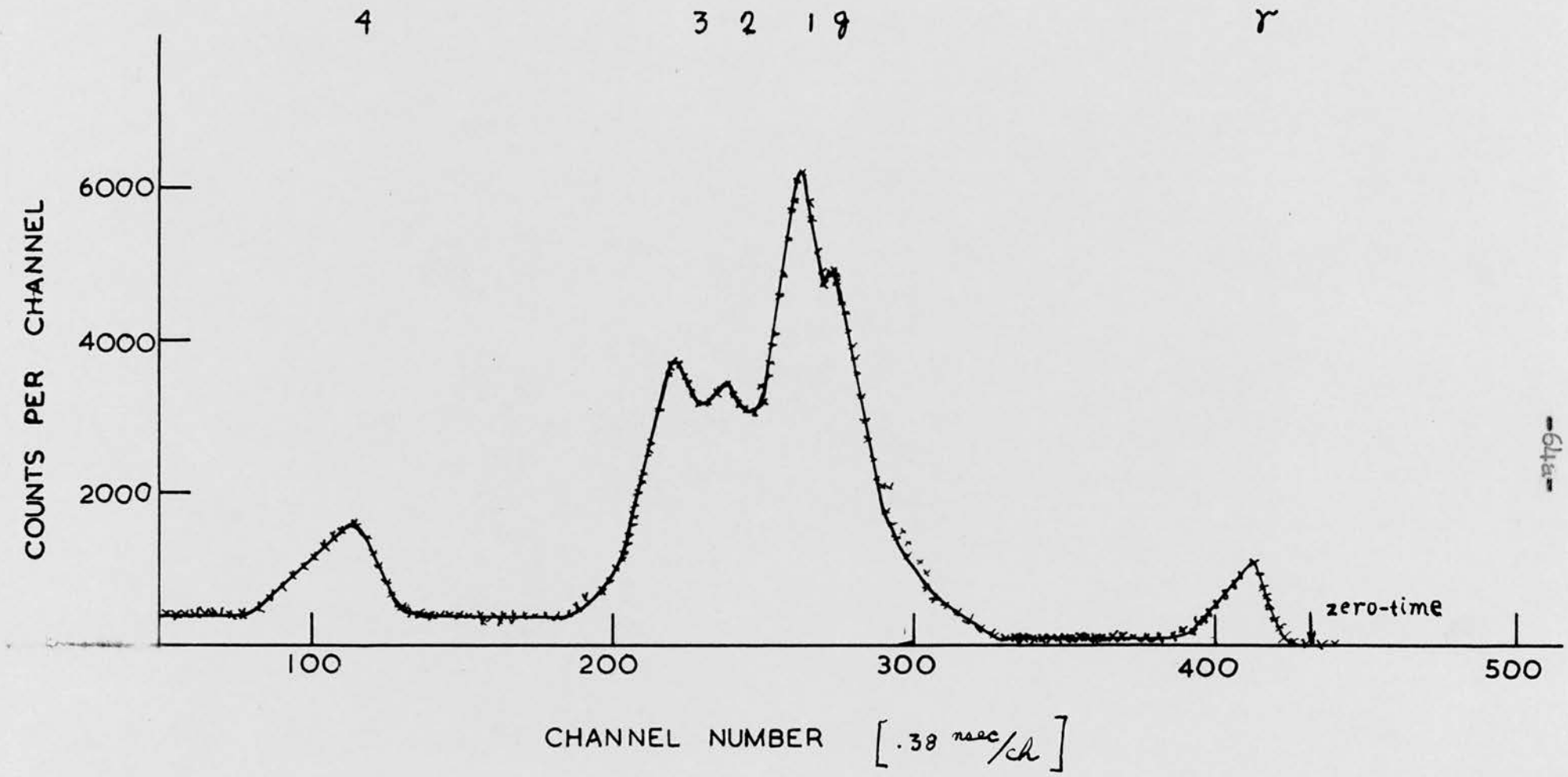

Fig. 42. $B^{9}_{e}(d,n)B^{10}$ REACTION, TIME-OF-FLIGHT SPECTRUM.

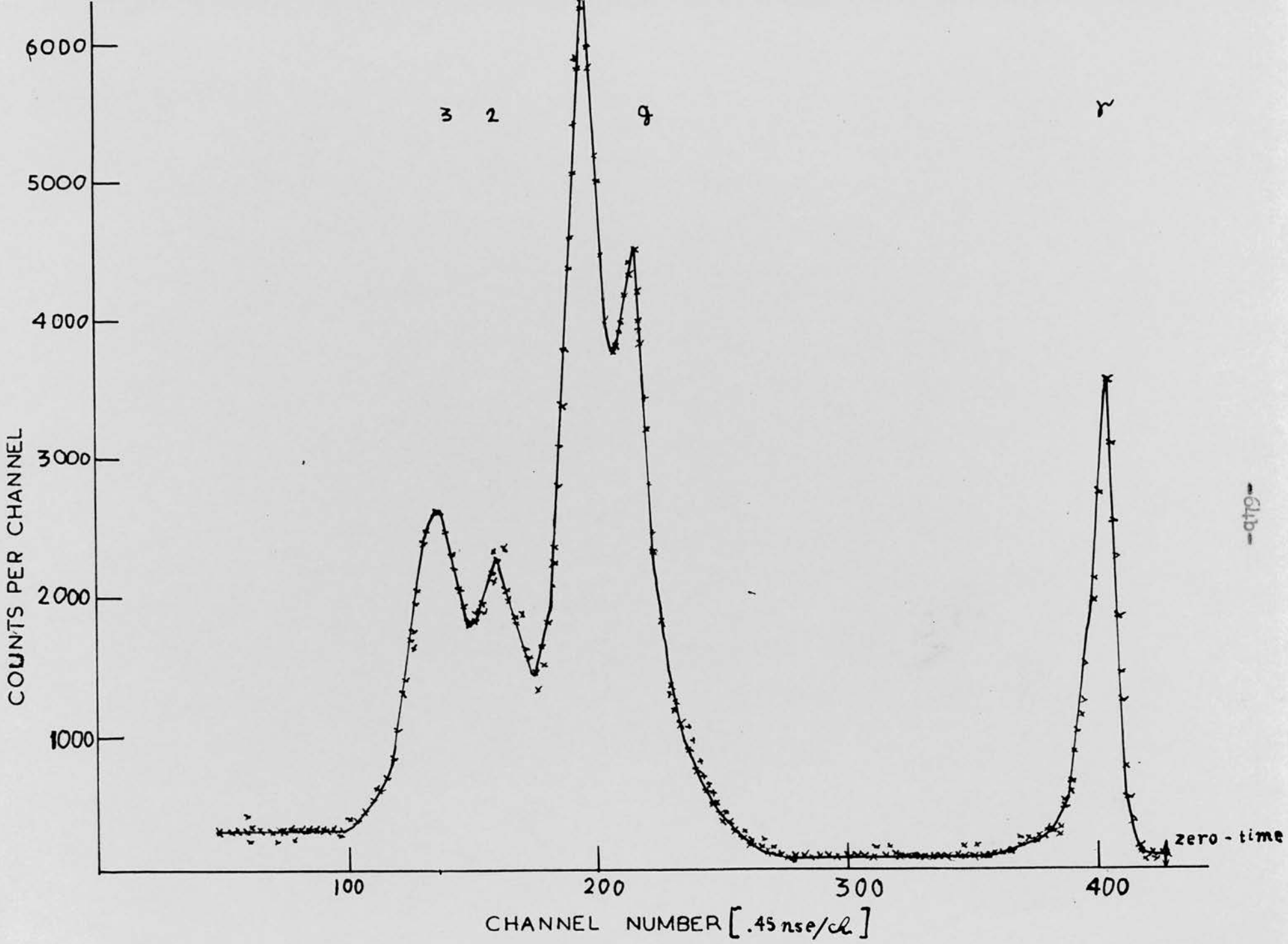

Fig. 43. $Be^{9}(d,n)B^{10}$ NEUTRON SPECTRUM.

the pulse shape discriminator was used and the detector was surrounded by a paraffin wax shield to protect against neutrons scattered from the walls. The necessary time of measurement to obtain the spectrum with good statistics was 30 minutes. The first small peak in this spectrum (Fig. 42) is due to the γ-rays which were not entirely eliminated by the pulse shape discriminator and therefore appear near the time zero in relation to other peaks. The neutron group corresponding to the $D(d,n)He^3$ reaction should be very near to the group associated with the second excited state of B^{10}. Because of that, and because of the very high yield from the $B_e^9(d,n)B^{10}$ reaction this group could not be noticed on the plotted spectrum. The peak to background ratio is large enough to show that there is no energy level at 2.86 Mev in B^{10}. The corresponding time-of-flight for neutrons feeding this level would be 100.10 nsec., for the above conditions. As could be seen from Fig. 42, the resolving time of the system was not sufficient to obtain good separation between different peaks corresponding to the different energy levels. In order to obtain a better separation the detector was moved to a distance of 3 meters from the target. Because of the high repetition rate of the ion bursts, a time-of-flight spectrum no wider than 180 nsec. can be examined,

and therefore the plotted spectrum (Fig. 43) consists of only the first four neutron groups. Any increase in distance between detector and target will cause the last peaks to appear in an erroneous position, thus limiting the distance between detector and target that can usefully be employed. The pulse duration was measured from the width at half maximum of the γ peak (Fig. 43) and was found to be of the order of 3.5 nsec.

7. Conclusion

The "Philips 1.2 Mev Cascade Generator", after the reconstruction of most of the electronic equipment in the terminal and the addition of the pulsed section, is able to produce either a d.c. or a pulsed beam. Prior to these alterations, particles could be accelerated to a maximum energy of 1 Mev with maximum current of 500 μA on the target. The beam diameter was of about 10 mm. Because of the new design of the focussing system, the accelerator is now able to produce the same d.c. current with a diameter of about 3 mm. In a pulsed operation it is possible to obtain bursts with duration of about 3 to 150 nsec, a peak current of about 500 μA, and a repetition rate of $4MH_z$. This has been proved by electronic measurements and various physical experiments. The long term stabilization factor of the accelerator's high voltage is about 5%, and as the time required for the particles to travel from the zero timing pick-up to the target, is of the order of 20 nsec., another time spread, of the order of 1 nsec, results. It seems, that even if a bunching magnet is added (see part 8) the minimum burst duration will not be reduced to less than 2 nsec, though the peak current will be increased by a factor of 10. On the other hand increasing the source r.f.

oscillator power, will increase the current by a factor of 2 or 3.

The time-of-flight spectrometer of the pulsed accelerator has a resolving time of better than 3 nsec., and this could be reduced to less than 1 nsec. by changing the pulse shaper used with the 56AVP photomultiplier.

The burst repetition rate is of the order of $4MH_z$. In low yield nuclear reaction experiments when the time-of-flight is shorter than the repetition period, a higher yield may be obtained simply by increasing the frequency of the deflector oscillator up to a maximum value of 15 MH_z. Reducing the frequency of the same oscillator will decrease the repetition rate, although it would then be necessary to increase the amplitude of the peak r.f. voltage in order to get the same burst duration. The amplitude is limited by the insulators used, so this method is impracticable. Another way or reducing the repetition rate is by means of deflector plates inserted before the target and supplied with a synchronized r.f. voltage of appropriate frequency. The disadvantage here, lies in the fact that the unused bursts will increase the γ-ray background and add a neutron group from the $D(d,n)He^3$ reaction.

As far as most experiments are concerned, the repetition rate is adequate but as explained above, it could be altered for specific

experiments if desired.

8. APPENDIX

The Bunching Magnet

The use of a bunching magnet to produce a pulsed beam was proposed by R.C. Mobley[3]. The principle involves the sweeping of the ion beam across the face of a magnet (Fig. 44) in such a way that the first particle leaving the deflector takes the longest path through the magnet and the last particle the shortest. Thus, all particles will arrive at a certain image point as a short pulse.

The time interval over which particles can be accepted for bunching is:

$$2\,tc = \frac{L_2 - L_1}{v} \qquad (54)$$

where $2tc$ - time of acceptance.

L_1 and L_2 are the shortest and longest path lengths.

v - velocity of particles.

It can be shown[33] that

$$L_2 - L_1 = \frac{\phi}{H.R} \qquad (55)$$

where ϕ = magnetic flux enclosed between L_1 and L_2

H = magnetic field

R = radius of curvature of the path in the magnetic field.

For a uniform field this becomes

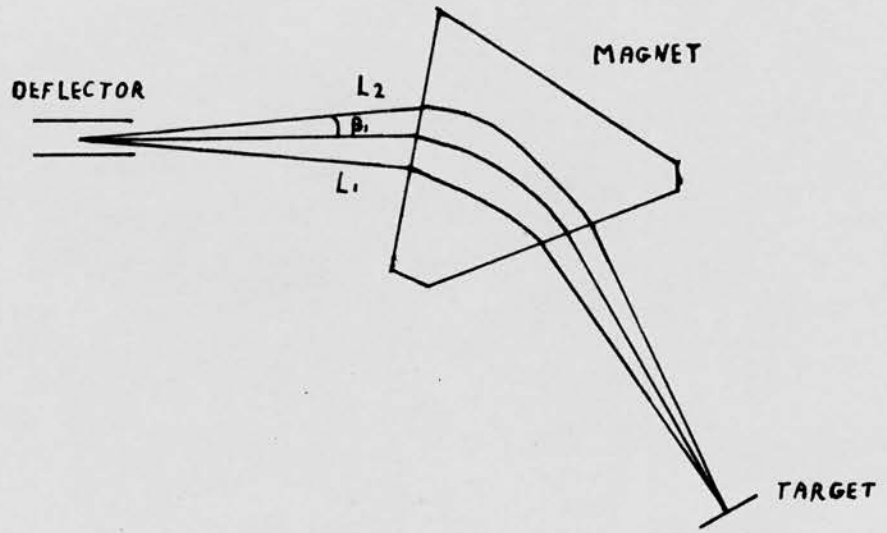

Fig. 44. SCHEMATIC REPRESENTATION OF A BUNCHING MAGNET.

$$L_2 - L_1 = \frac{A}{R} \qquad (56)$$

where A = area of pole face.

The magnetic flux is given by

$$\phi = (L_2 - L_1)\frac{c}{q}\, mv \qquad (57)$$

where q = charge on a particle

mv = momentum of a particle

c = velocity of light.

For best results the deflection angle θ of the magnet should be between 60 and 90°.

The following is a calculation for a 90° bunching magnet (Fig. 45), for the "Philips 1.2 Mev Electrostatic Accelerator". The calculation is based on the one given by R.E. Holland(33) 37).

The main equations are summarized below.

$$y_1 = 2\rho \cot 45^\circ \cos \varepsilon \qquad (58)$$

The distance from magnet to target, ℓ_2, is equal to the distance ℓ_1 between the deflector plates and magnet

$$\ell_2 = 2R \qquad (59)$$

The maximum input deflection

$$\beta_o = \frac{v_o}{4\omega R} \qquad (60)$$

The maximum input deflection accepted is

$$\beta_c = \frac{t_c v_o}{4R} \qquad (61)$$

The pulse width t_a is equal to :

$$t_a = \frac{2fc}{K} \qquad (62)$$

where K is the bunching ratio.

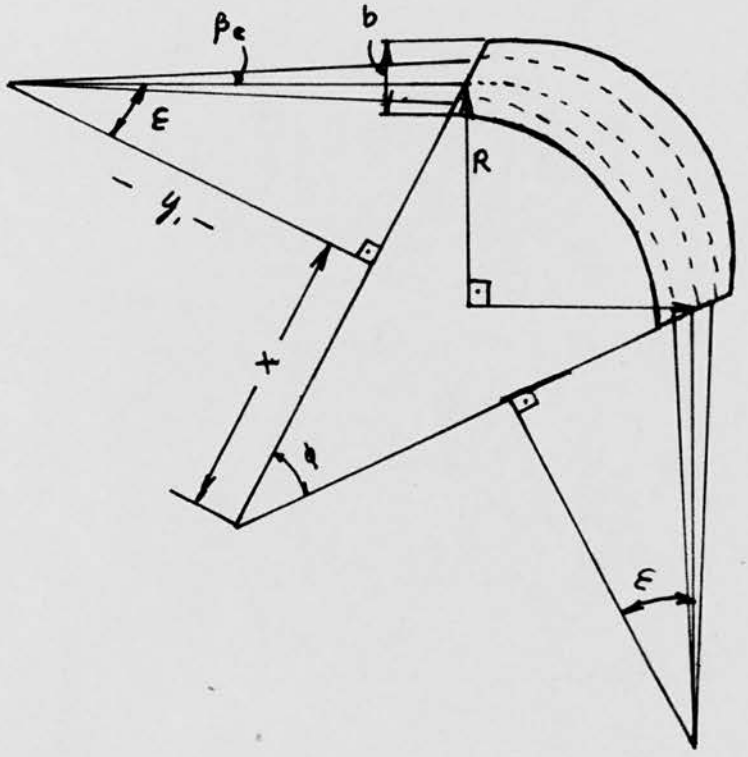

Fig. 45. THE BUNCHING MAGNET.

Assuming a deuteron beam of 600 keV deflected by a bunching magnet, radius R° of 30 cm. with an acceptance time of $2t_c$ = 10 nsec., and a r.f. deflection frequency of 8 MH_z, the other parameters according to the last equations would have the following values:

$$\ell_1 = \ell_2 = 60 \text{ cm.}$$
$$\beta_o = 0.145 \text{ rad.}$$
$$t_a = 0.8 \text{ nsec.}$$
$$B = 6100 \text{ gauss.}$$
$$A = 261 \text{ cm.}^2$$
$$\beta_c = 0.036 \text{ rad.}$$

The maximum deflection of the accepted beam would be

$$D = \ell_2 \beta_c = 2.16 \text{ cm.} \qquad (53)$$

The minimum magnet width should be twice the beam deflection, for safety.

$$b = 7 \text{ cm.}$$

The maximum deflection of the beam would be

$$y = \ell_2 \cdot \beta_o = 8.7 \text{ cm.} \qquad (54)$$

Assuming deflector plates of 15 cm. long, 1 cm. apart, the peak r.f. voltage required on the plates according to (12), will be of 20 kV when the frequency is 8MH_z.

The bunching magnet can change an accepted d.c. beam into a pulsed one. The main disadvantage is that the rest of the beam will hit the magnet

and produce a large background. In order to prevent an unnecessary background the bunching magnet should accept a pulsed beam with a burst duration of 10 nsec., which was the time of acceptance in the above calculation. That could be achieved if the r.f. voltage supplied to the deflector plates is synchronized with the time of arrival of the pulses. A pick-up (Fig. 46) located after the resolving magnet produces a voltage pulse whenever the pulsed beam passes through. The output is amplified and fed into a harmonic oscillator. This generator output should be a 8 MH_z sin r.f. voltage with an adjustable amplitude up to a maximum of 25 kV. A variable delay in front of the harmonic oscillator will adjust the r.f. phase so that the r.f. voltage will reach its zero potential whenever the pulsed beam is passing. Before reaching the target the beam is passed through a second pick-up to give the zero-timing pulse for the experiment. The two pick-ups and the appropriate amplifiers could be of the same type as the one described in part 5.

A few factors limit the minimum burst duration.

1. Energy spread.

Assuming an acceleration energy of 600 keV,

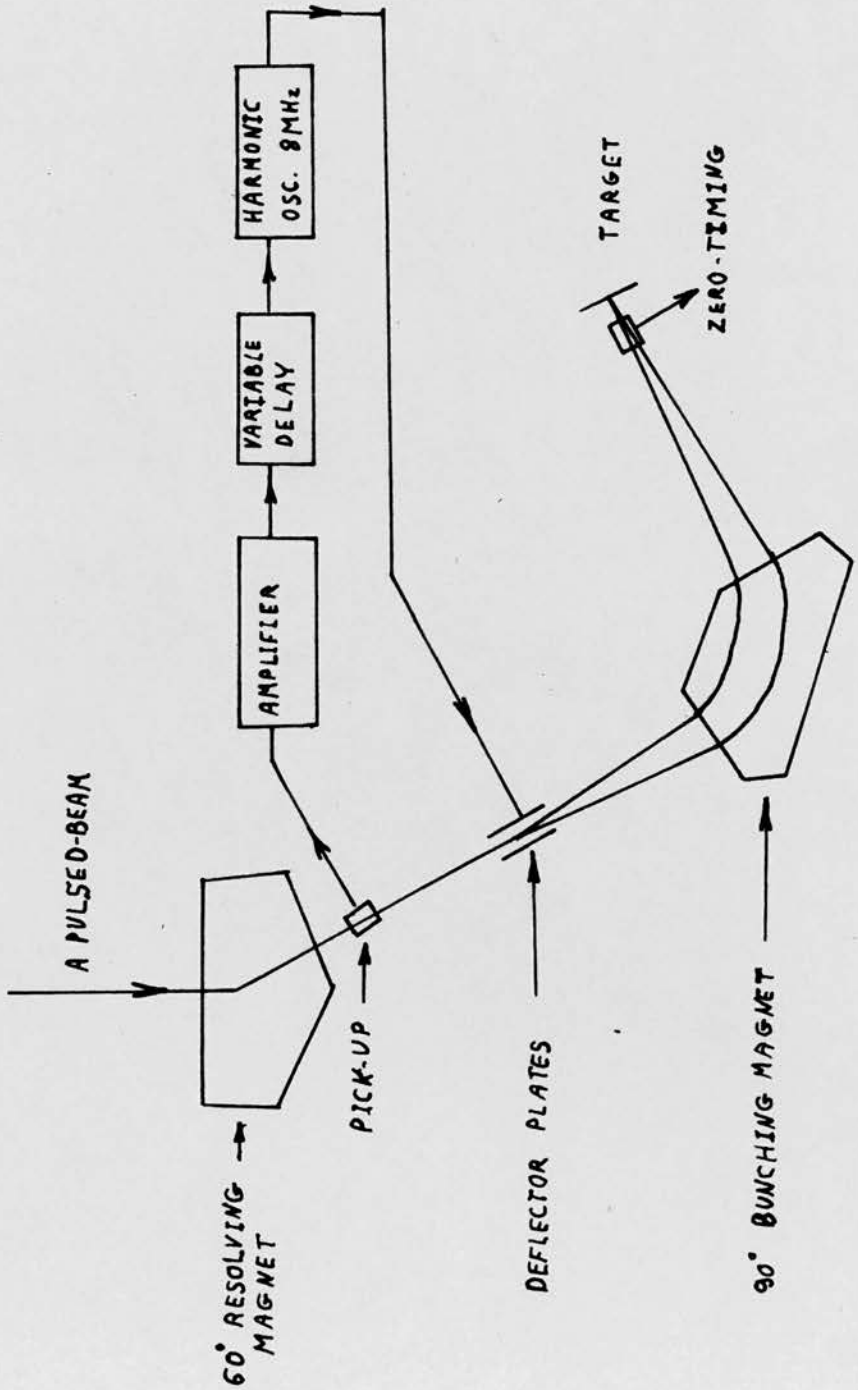

Fig. 46. BLOCK DIAGRAM OF THE BUNCHING MAGNET ASSEMBLY.

the velocity of deuterons is $v_o \approx 8.10^8$ cm./sec. Assuming a velocity spread, within the burst, of v_o (about 0.1% in our case) the corresponding spread in time will be:

$$\Delta t = \frac{L}{\Delta v_o} \qquad (65)$$

where L = path length of particle between the resolving magnet and the target. In the case described $\Delta t \approx 0.4$ nsec. The velocity spread is due mainly to the energy spread caused by the deflector plates before the bunching magnet, and to a lesser extent by the deflector plates in the terminal.

2. Beam diameter.

Because of the finite beam diameter, the two extreme rays will have a difference in path length (33)

$$\Delta L = \theta . d \qquad (66)$$

where θ = deflection of median ray ($\frac{\pi}{2}$ in our case),

d = diameter of the beam.

Thus, there will be a time spread of

$$\Delta t = \frac{\Delta L}{v_o} \qquad (67)$$

For the same conditions of beam as described above and assuming a beam diameter of 4 mm., the

time spread will be $\Delta t \approx 0.8$ nsec.

It is possible to pass the beam through a focussing lens and so to reduce the diameter of the beam. However in our case the target room is too small for this possibility to be practicable.

3. Beam divergence.

Because the beam is not parallel, a spread in time of arrival results. This spread limits the maximum bunching factor K. Assuming a beam divergence of 0.005 rad, according to R.E. Holland[33], the maximum K is of the order of K = 9-10 for the above condition.

If a bunching magnet were added to the "Philips High Voltage Generator" it can be estimated from the above that the bursts produced would have a minimum duration of between 1 and 1.5 nsec., with a bunching factor of about 9. The bursts supplied by the accelerator should have a duration of about 10 nsec. The peak current after bunching would be about 9 times the peak current of the bursts arriving from the accelerator.

ACKNOWLEDGEMENTS

I wish to thank Professor N. Feather, F.R.S., for enabling me to carry out this work at the Edinburgh University Physics Department, and to Mr. R.M. Sillitto, my superviser, for the helpful comments and support throughout the work. I thank Mr. R.B. Galloway for his support and for the exceptionally good help and advice. I thank Dr. G. Bradford and Mr. D. Vass for the helpful discussions we held throughout this work.

During my research I held a Junior Fellowship from the University. I thank Professor N. Feather and the University of Edinburgh for this financial assistance. The work was supported by an equipment grant from the D.S.I.R., to whom I give my thanks.

I thank Mr. W.B. Wilson for his help in ordering the many components and equipment needed for the research. My thanks go too to Mr. A. Headridge and the other workshop technicians for their great help in the construction of all the mechanical components, and to Mr. H.T. Napier for his valuable technical assistance.

REFERENCES

1. C.M. Turner & S.D. Bloom, Rev. Sci. Instr. 29 (1958) 480.
2. K.R. Spangenberg, Vacuum Tubes, McGraw-Hill, New York, 1948.
3. R.C. Mobley, Phys. Rev. 88 (1952) 360.
4. J.B. Marian and J.L. Fowler, Fast Neutron Physics, Part I, Interscience Publishers, New York, 1960.
5. G.C. Neilson and W.K. Dowson, Rev. of Sci. Instr. 30 (1959) 963.
6. V.E. Parker & R.E. King, Bull. Am. Phys. Soc. 1 (1956) 70.
7. L.E. Beghian & M.K. Saloma, Nucl. Instr. 17 (1962) 181.
8. E.C. Fellows & B.A. Bumford, Nucl. Inst. 22 (1963) 351.
9. Richard J. Cannon, Nucl. Instr. 11 (1961) 122.
10. L. Cranbery, R.A. Fernald and E.F. Shrader, Nucl. Instr. 12 (1961) 335.
11. A.K. Ganguly & A. Bakhru, Nucl. Instr. 21 (1963) 56.
12. M. Sanley Livingston & J.P. Blewett, Particle Accelerators, McGraw-Hill, New York (1962).
13. V.E. Cosslett, Introduction to Electron Optics, Oxford, At The Clarendon Press (1946).
14. T.K. Fowler and W.M. Good, Nucl. Instr. 7 (1960) 245.
15. D. Maydan, A Time-To-Amplitude Converter for Use With A Pulsed Accelerator, Nucl. Instr., in press.

REFERENCES (Contd.)

16. C.W. Williams & J.H. Neiler, I.R.E. Transactions on N.S. 5 (1962) 1.

17. R.E. Green & R.E. Bell, Nucl. Instr. 3 (1958) 127.

18. Arthur E. Bjerke. Nucl. Instr. 15 (1962) 249.

19. P.R. Orman, Nucl. Instr. 21 (1963) 121.

20. R.B. Owen, I.R.E. Transactions on N.S. 3 (1958) 198.

21. R. Batchelor, W.B. Gilboy, A.D. Purnall & T.H. Toube, Nucl. Instr. 8 (1960) 146.

22. J.D. Seagrave, Neutron Source Handbook, Loss Alamos, Scientific Lab., Univ. of Cal. (1957).

23. Energy Levels of Light Nuclei, National Academy of Science.

24. D. Vass, Private communication, Later to be published as a Ph.D. thesis.

25. C.H. Paris & P.M. Endt, Physica 20 (1954) 585.

26. Dyer & Bird, Aust. J. Phys. 6 (1953) 45.

27. Genin, C. Rendus 246 (1958) 1028.

28. Reid, Proc. Phys. Soc. 67A (1954) 466.

29. Shpetnyi, Soviet Physics, J.E.T.P. 5 (1957) 357.

30. Galloway & Sillitto, Proc. Roy. Soc. Edinburgh 65A (1961) 247.

31. G. Bradford, Ph.D. Thesis, Edinburgh, (1962).

32. R.A. Coombe & J. Walker, Univ. of Birmingham (1962) Paper No. 12.

33. R.E. Holland, Nucl. Instr. 12 (1961) 103.